Computer Modeling in Engineering & Sciences

Tech Science Press

Doi:10.32604/cmes.2025.070268

ARTICLE

Modeling Hepatitis B and Alcohol Effects on Liver Cirrhosis Progression

Zia Ur Rahman[1], Nigar Ali[1,2], Dragan Pamucar[3], Imtiaz Ahmad[1,2], Haci Mehmet Baskonus[2,*], Naseer Ul Haq[1] and Zeeshan Ali[4]

[1]Department of Mathematics, University of Malakand, Chakdara Dir(L), 18000, Khyber Pakhtunkhwa, Pakistan
[2]Department of Mathematics and Science Education, Faculty of Education, Harran University, Sanliurfa, 63150, Turkey
[3]Széchenyi István University, Egyetem tér 1, Gyor, 9026, Hungary
[4]Department of Information Management, National Yunlin University of Science and Technology, Douliu, 640301, Taiwan

*Corresponding Author: Haci Mehmet Baskonus. Email: hmbaskonus@gmail.com

Received: 11 July 2025; Accepted: 24 November 2025; Published: 29 January 2026

ABSTRACT: Hepatitis B Virus (HBV) infection and heavy alcohol consumption are the two primary pathogenic causes of liver cirrhosis. In this paper, we proposed a deterministic mathematical model and a logistic equation to investigate the dynamics of liver cirrhosis progression as well as to explain the implications of variations in alcohol consumption on chronic hepatitis B patients, respectively. The intricate interactions between liver cirrhosis, recovery, and treatment dynamics are captured by the model. This study aims to show that alcohol consumption by Hepatitis B-infected individuals accelerates liver cirrhosis progression while treatment of acutely infected individuals reduces it. We proved that a unique solution of the proposed model exists, which is positive and bounded. Using the next-generation matrix approach, two basic reproductive numbers $\mathscr{R}_{A_0}$ and $\mathscr{R}_{A_{max}}$ are calculated to identify future recurrence. The equilibrium points are calculated, and both equilibria are proved locally and globally asymptotically stable when $\mathscr{R}_0$ is below and above one, respectively. It is shown that bifurcation exists at $\mathscr{R}_0 = 1$ and a detailed proof for forward bifurcation is given. Furthermore, we performed the sensitivity analysis of the model parameters on $\mathscr{R}_0$. For the confirmation of analytical work, we performed numerical simulations, and the results indicate that the treatment and the inhibitory effects reduce the risk of developing liver cirrhosis in individuals, while heavy alcohol consumption accelerates markedly the liver cirrhosis progression in patients with chronic hepatitis B.

KEYWORDS: Liver cirrhosis; deterministic model; saturated incidence rate; stability; forward bifurcation

1 Introduction

The late stage of liver disease, known as liver cirrhosis, occurs when the liver organ fails to function correctly due to the possible transformation of healthy liver tissue into scar tissue caused by alcohol processing stress or viral infections. In the world, cirrhosis is responsible for one million fatalities annually, indicating its significant morbidity and mortality rates [1]. Ultimately, a chronic or continual injury causes the liver to slowly languish and become incapable of functioning properly. A distinctive feature of the liver is its ability to regenerate; however, this process is also inhibited by liver cirrhosis. Hepatitis B and C virus infections, prolonged alcohol consumption, other liver illnesses and disorders can all lead to cirrhosis. The risk of developing cirrhosis is higher in those with chronic viral infections [2]. Although before the extensive liver damage, the liver cirrhosis has no apparent symptoms. Hepatitis B is a major worldwide health concern, caused by a virus called hepatitis B. Fever, fatigue, joint pain, loss of appetite, nausea, vomiting, and jaundice may occur two weeks later as symptoms. An incubation period of 45–180 days (average 60–90

Copyright © 2026 The Authors. Published by Tech Science Press.
This work is licensed under a Creative Commons Attribution 4.0 International License, which permits unrestricted use, distribution, and reproduction in any medium, provided the original work is properly cited.

days) meant that many of the infected would not experience symptoms. Mother-to-child transmission and contact with contaminated bodily fluids such as blood, saliva, vaginal secretions, and semen are potential transmission modes [3,4]. In 2022, the World Health Organization estimates that 254 million individuals have a chronic hepatitis B infection, with 1.2 million new cases reported annually. An estimated 1.1 million people died mostly from cirrhosis and hepatocellular carcinoma (HCC) as a result of hepatitis B in 2022 [5]. Another significant risk factor for the development of chronic liver cirrhosis is heavy alcohol use, with 38% of adults over 15 years, consuming more than 17 liters of pure alcohol per year [6]. The prevalence of cirrhosis is approximately 10 to 20 percent of heavy drinkers after ten or more years, especially in individuals taking at least 50 grams of pure alcohol daily over 10 to 20 years, and there is a high degree of risk of fast liver destruction when alcohol intake is combined with HBV infection [7]. However, a lot of studies have demonstrated that the risk of developing cirrhosis is not increased if people do not consume more than 50 grams of pure alcohol daily. Consuming more than 50 grams of pure alcohol per day, however, speeds up the development towards liver cirrhosis in chronic hepatitis B carriers for both men as well as women. It is poisonous and fatal if a person weighing 60 kg takes in more than 300 grams of alcohol daily [8–10]. Hepatitis B effective vaccine available with 95% effective antibodies [11]. Chronic infection treatment is crucial to reduce the risk of severe problems like liver cancer or cirrhosis. Treatment duration varies depending on the genotype and medication used, ranging from six months to a year [12].

In studying the dynamical behavior of epidemic models, the incidence rates play a vital role. Capasso and Serio [13], for the first time, proposed the idea of saturation incidence rate $\frac{\beta(\mathbb{A})\mathbb{S}\mathbb{I}}{1+\alpha_2\mathbb{I}}$. In a population that is completely susceptible to the illness, $\frac{\beta(\mathbb{A})\mathbb{I}}{1+\alpha_2\mathbb{I}}$ achieves the saturation level when $\mathbb{I}$ grows and $\alpha_2\mathbb{I}$ measures the force of infection after entering the disease. In this incidence rate $\frac{1}{1+\alpha_2\mathbb{I}}$ measures the inhibitory impact of behavioral changes in susceptible people when the number of infected people rises or the crowding effect of infective individuals. Compared to bilinear, the saturated incidence rate is more general.

The dynamical behavior of infectious illnesses, such as cholera, liver cirrhosis, Hepatitis B infection, and others, is commonly studied using mathematical models. Apart from modelling of infectious diseases, various research has also been done for anticancer medication and locating numbers [14,15]. Mathematical models are considered to be the tool helping to discuss hypotheses, verify the experiments, and simulate the dynamics of complex objects. Zhou and Fan [16] created an SIR (Susceptible-Infective-Recovered) model for susceptibility, infection, and recovery analysis to evaluate human behavior during medical resource shortages. Ilhan and Sahin have used the Morgan-Voyce collocation method (M-VCM) to determine the approximate solution of the SIR model with the vaccination effect. Their paper provides an alternative criterion of the certainty of the approximate solutions. They primarily tried to determine the exact solutions of the SIR model of vaccination [17]. Researchers have developed multiple models to study relationships between alcohol abuse patterns alongside cirrhosis evolution and hepatitis B virus infection processes. Park et al. [18] investigated the factors linked to alcohol consumption among Hepatitis B carriers in Korea and concluded that hazardous alcohol consumption is defined as consuming more than sixty grams of alcohol on one occasion for males or forty grams of alcohol on several occasions for females. A continuous and a discrete mathematical model were developed by Khajji et al. [19] to investigate the dynamical behavior of alcohol use and the effects of both public and private addiction treatment centers. By utilizing a mathematical model and an optimum control technique [20,21] elucidated the dynamics of infectious diseases and came to the conclusion that the illness may be controlled by vaccination and treatment. Zhou et al. [22] compared moderate and excessive drinking and came to the conclusion that moderate alcohol consumption has no discernible impact on the progression of liver cirrhosis, whereas excessive drinking causes liver inflammation in patients with chronic Hepatitis B infection, ultimately accelerating the progression of the disease. A mathematical model developed by Dano et al. [23], consisting of four classes, namely susceptible, acutely

infected, cirrhotic, and recovered, with a logistic model to study the combined effect of Hepatitis B infection and heavy alcohol consumption on liver cirrhosis progression dynamics.

The novelty of our research is considering the effect of exposed and treated classes. Since Hepatitis B has a latent phase, and treatment effects. With the inclusion of the exposed class, a latent period is introduced, which delays the transmission of individuals into the acutely infected class. We assumed that a fraction of individuals move from the exposed to the recovered compartment directly. The treated class is included to model the impact of medical interventions, which helps in analyzing how treatment reduces the infectious (both acutely infected and cirrhotic) population and reduces the progression to liver cirrhosis. Moreover, the existence of a unique solution for the proposed model is examined, which is ignored in most of the papers. Furthermore, we used a saturated incidence rate to study the saturation effects. Two basic reproductive numbers are calculated when the minimum and maximum amount of pure alcohol is consumed, respectively. The 3D analysis of these basic reproductive numbers are also carried out. To the author's utmost knowledge, no one has yet considered the same.

We organized this research study as follows. The model formulation, description, as well as associated assumptions are presented in Section 2. In Section 3, the qualitative analysis of the proposed model is presented. That is, the solution is of existence, uniqueness, positivity, as well as boundedness. Moreover, the feasible region is defined, equilibrium points, the basic reproductive number with 3D-type simulation, and local and global asymptotic stability at equilibria are calculated. In Section 4, the bifurcation phenomena are analyzed, where we proved the existence of forward bifurcation of the proposed model. The sensitivity analysis is carried out in Section 5, while the numerical simulations are explored in Section 7, and the conclusion is presented in Section 8.

2 Model Formulation

The total human population is denoted by $\mathbb{N}(t)$ and partitioned into six different compartments namely the susceptible, exposed, acutely infected, liver cirrhotic, treated and recovered denoted by $\mathbb{S}(t)$, $\mathbb{E}(t)$, $\mathbb{I}(t)$, $\mathbb{C}(t)$, $\mathbb{T}(t)$ and $\mathbb{R}(t)$, respectively. The susceptible individuals $\mathbb{S}(t)$ include those who are at risk of becoming infected but have not yet been infected at time t. People in the susceptible group are not immune to a possible infection. The exposed compartment $\mathbb{E}(t)$ includes those individuals who are infected but not yet infectious, meaning that they are in the incubation period, which implies that in their bodies the pathogen is present and replicating, but they are not capable of transmitting the disease to others. The population with acute infection $\mathbb{I}(t)$ is those who are currently infected with the disease, have developed a robust enough immunity to eradicate the disease from their bodies, and have the ability to transmit the disease to others. People with liver cirrhosis $\mathbb{C}(t)$ are asymptomatic infection individuals with end-stage liver disease who are capable of spreading the disease at any time t. Treated compartment $\mathbb{T}(t)$ includes those individuals who do not have enough immunity to clear the disease from their bodies; therefore, they are treated successfully, and they are capable of transmitting the disease to other people at any time t. The recovered class $\mathbb{R}(t)$ includes those individuals who gained enough immunity and eradicated the disease. The sub-model of alcohol consumption in our Hepatitis B virus transmission model is nonlinear, and this is because of the effects of behavioral saturation. This type of modeling has been followed in the recent works on hemodynamic modelling [24], where the blood flow through the arteries' dynamics is described by the non-linear wave equations with the Bernoulli-type terms. These models make clear the fact that, in both fluid flow and behavioral epidemiology, nonlinearities play a critical role in relation to adequately describing biological phenomena.

We impose the following assumptions on the proposed model:

- $\mathfrak{a}_1$. The recruitment to the susceptible population is purely due to new births.
- $\mathfrak{a}_2$. Saturated incidence rate is considered.
- $\mathfrak{a}_3$. The disease transmission coefficient $\beta(\mathbb{A}) = \beta_0 + \beta_1 \left(\frac{\mathbb{A}(t) - A_0}{A_{max}} \right)$ is dependent upon variations in alcohol intake among Hepatitis B infected individuals.
- $\mathfrak{a}_4$. The recovered population has permanent immunity.
- $\mathfrak{a}_5$. Individuals with successful vaccination goes to the recovered class.
- $\mathfrak{a}_6$. The vaccination may result in temporary immunity.

The model accounts for individual variations in alcohol metabolism through the dynamic transmission coefficient $\beta(\mathbf{A})$, which adjusts based on alcohol intake levels. By incorporating a logistic growth term for alcohol consumption and a saturation incidence rate, the framework implicitly captures the nonlinear effects of alcohol metabolism on Hepatitis B progression. While the model does not explicitly include genetic or physiological factors, the alcohol-dependent transmission rate and saturation effects provide a proxy for metabolic variability, ensuring that the progression dynamics reflect the heterogeneity observed in real-world populations. Future refinements could integrate explicit metabolic parameters to further enhance the model's precision.

The proposed model is given by the following system of differential equations, and Fig. 1 represents its schematic diagram, while parameters of the model are listed in Table 1 with their descriptions, values, and sources.

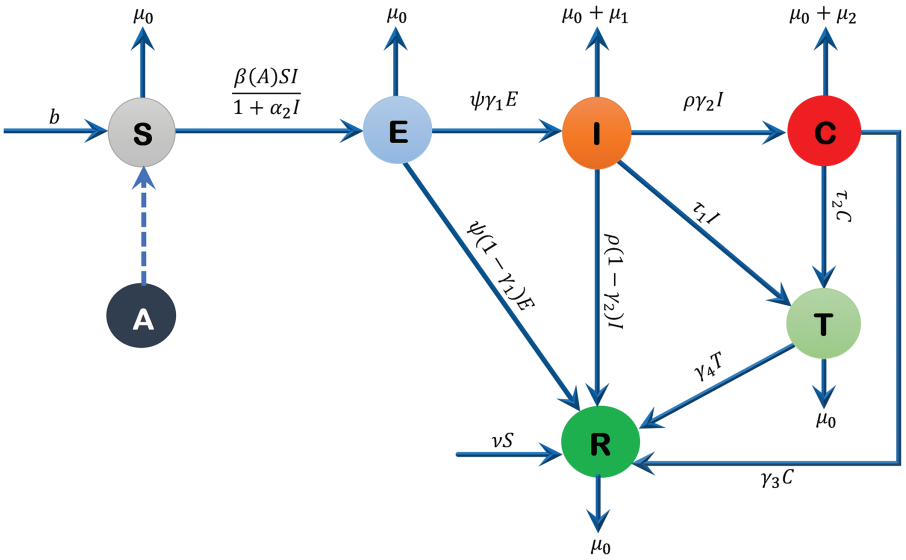

Figure 1: Flow diagram of the formulated model

Table 1: Model parameters, their descriptions, values and sources

Symbols	Descriptions	Value (year^{-1})	Reference
b	Recruitment rate	0.5800	[25]
ν	New born infants vaccination rate	0.0020	[25]
μ_0	Natural death rate	0.0300	[8]

(Continued)

Table 1 (continued)

Symbols	Descriptions	Value (year^{-1})	Reference
α_2	Saturation parameter	0.0050	[Assumed]
β_0	Baseline transmission rate of liver cirrhosis	0.0050	[8]
β_1	Incremental rate of pure alcohol consumption	0.0120	[Assumed]
r	Alcohol consumption growth rate	0.0650	[23]
A_0	Daily min. alcohol consumption (g/day)	20	[7,26]
A_{max}	Daily max. alcohol consumption (g/day)	75	[10]
μ_1	Mortality rate due to disease in acutely infected class	0.0020	[8]
μ_2	Mortality rate due to liver cirrhosis in cirrhotic class	0.0020	[23]
ψ	Transmission rate from exposed to infected class	0.0500	[Assumed]
γ_1	Fraction of exposed individuals who becomes acutely infected	0.6000	[Assumed]
ρ	Transmission rate from acutely infected to cirrhotic class	0.0600	[Assumed]
γ_2	Fraction of acutely infected individuals who becomes liver cirrhotic	0.9000	[Assumed]
τ_1	Treatment rate of acutely infected individuals	0.0100	[Assumed]
τ_2	Treatment rate of liver cirrhotic individuals	0.0300	[Assumed]
γ_3	Recovery rate of liver cirrhotic individuals due to self-immunity	0.0300	[2]
γ_4	Recovery rate of individuals from treatment class	0.0300	[Assumed]

Note: All rate parameters are expressed in year^{-1} units. Alcohol quantities (A_0, A_{max}) are in grams of pure alcohol per day (g/day).

$$
\begin{cases}
\frac{d\mathbb{S}(t)}{dt} &= b - \frac{\beta(\mathbb{A})\mathbb{S}(t)\mathbb{I}(t)}{1+\alpha_2\mathbb{I}(t)} - (\nu+\mu_0)\mathbb{S}(t),\\
\frac{d\mathbb{E}(t)}{dt} &= \frac{\beta(\mathbb{A})\mathbb{S}(t)\mathbb{I}(t)}{1+\alpha_2\mathbb{I}(t)} - (\psi+\mu_0)\mathbb{E}(t),\\
\frac{d\mathbb{I}(t)}{dt} &= \psi\gamma_1\mathbb{E}(t) - (\rho+\tau_1+\mu_0+\mu_1)\mathbb{I}(t),\\
\frac{d\mathbb{C}(t)}{dt} &= \rho\gamma_2\mathbb{I}(t) - (\tau_2+\gamma_3+\mu_0+\mu_2)\mathbb{C}(t),\\
\frac{d\mathbb{T}(t)}{dt} &= \tau_1\mathbb{I}(t) + \tau_2\mathbb{C}(t) - (\gamma_4+\mu_0)\mathbb{T}(t),\\
\frac{d\mathbb{R}(t)}{dt} &= \psi(1-\gamma_1)\mathbb{E}(t) + \rho(1-\gamma_2)\mathbb{I}(t) + \nu\mathbb{S}(t) + \gamma_3\mathbb{C}(t) + \gamma_4\mathbb{T}(t) - \mu_0\mathbb{R}(t),\\
\frac{d\mathbb{A}(t)}{dt} &= r(\mathbb{A}(t)-A_0)\left(1-\frac{\mathbb{A}(t)}{A_{max}}\right),
\end{cases}
\tag{1}
$$

with initial conditions:

$$\mathbb{S}(0) > 0, \qquad \mathbb{E}(0) \geq 0, \qquad \mathbb{I}(0) \geq 0, \qquad \mathbb{C}(0) \geq 0, \qquad \mathbb{T}(0) \geq 0, \qquad \mathbb{R}(0) \geq 0, \quad \mathbb{A}(0) \geq 0.$$

The transmission function $\beta(A)$ incorporates alcohol consumption due to its significant biological and behavioral impact on Hepatitis B dynamics, despite Hepatitis B being primarily blood-borne. Chronic alcohol consumption exacerbates liver damage, increases viral replication, and weakens immune responses, leading to higher viral loads in transmissible bodily fluids such as blood and semen. This biological mechanism is supported by studies such as Ganesan et al. [7], who demonstrated that alcohol accelerates Hepatitis B progression by promoting viral persistence and liver fibrosis. Furthermore, alcohol use is associated with riskier behaviors (e.g., unsafe injections or sexual practices), indirectly amplifying transmission rates. The function $\beta(A) = \beta_0 + \beta_1 \left(\frac{A(t)-A_0}{A_{\max}}\right)$ quantifies this relationship, where β_0 represents the baseline transmission rate and β_1 captures the incremental risk from alcohol. This formulation aligns with clinical evidence and ensures the model reflects the synergistic effects of alcohol and Hepatitis B on liver cirrhosis progression.

The model accounts for the threshold alcohol consumption required to significantly impact Hepatitis B transmission rates through the transmission coefficient $\beta(\mathbf{A})$, defined as $\beta(\mathbf{A}) = \beta_0 + \beta_1 \left(\frac{\mathbf{A}(t)-\mathbf{A}_0}{A_{\max}}\right)$. Here, β_0 represents the baseline transmission rate without alcohol, while β_1 scales the additional risk due to alcohol consumption. The logistic growth of alcohol consumption, governed by $\frac{d\mathbf{A}}{dt} = r(\mathbf{A}(t) - \mathbf{A}_0)\left(1 - \frac{\mathbf{A}(t)}{A_{\max}}\right)$, ensures that $\mathbf{A}(t)$ remains bounded between $\mathbf{A}_0$ and $A_{\max}$. This formulation captures the saturation effect of alcohol on transmission rates, reflecting empirical observations that excessive alcohol intake accelerates Hepatitis B progression. The sensitivity analysis further confirms the pronounced impact of β_1 on $\mathscr{R}_0$, particularly when $\mathbf{A}(t)$ exceeds $\mathbf{A}_0$, aligning with clinical evidence on the synergistic effects of alcohol and Hepatitis B.

3 Qualitative Analysis

3.1 Existence and Uniqueness of the Solution

In this subsection, we prove that the solution to system (1) exists and is unique.

Theorem 1: *The solution of the model (1) equations together with the initial conditions exists in* $\mathbb{R}^7_+$.

Proof: The *RHS* of model (1) can be written as follows,

$$\mathfrak{F}_1(\mathbb{S},\mathbb{E},\mathbb{I},\mathbb{C},\mathbb{T},\mathbb{R},\mathbb{A}) = b - \frac{\beta(\mathbb{A})\mathbb{S}(t)\mathbb{I}(t)}{1+\alpha_2\mathbb{I}(t)} - (\nu+\mu_0)\mathbb{S}(t),$$

$$\mathfrak{F}_2(\mathbb{S},\mathbb{E},\mathbb{I},\mathbb{C},\mathbb{T},\mathbb{R},\mathbb{A}) = \frac{\beta(\mathbb{A})\mathbb{S}(t)\mathbb{I}(t)}{1+\alpha_2\mathbb{I}(t)} - (\psi+\mu_0)\mathbb{E}(t),$$

$$\mathfrak{F}_3(\mathbb{S},\mathbb{E},\mathbb{I},\mathbb{C},\mathbb{T},\mathbb{R},\mathbb{A}) = \psi\gamma_1\mathbb{E}(t) - (\rho+\tau_1+\mu_0+\mu_1)\mathbb{I}(t),$$

$$\mathfrak{F}_4(\mathbb{S},\mathbb{E},\mathbb{I},\mathbb{C},\mathbb{T},\mathbb{R},\mathbb{A}) = \rho\gamma_2\mathbb{I}(t) - (\tau_2+\gamma_3+\mu_0+\mu_2)\mathbb{C}(t),$$

$$\mathfrak{F}_5(\mathbb{S},\mathbb{E},\mathbb{I},\mathbb{C},\mathbb{T},\mathbb{R},\mathbb{A}) = \tau_1\mathbb{I}(t) + \tau_2\mathbb{C}(t) - (\gamma_4+\mu_0)\mathbb{T}(t),$$

$$\mathfrak{F}_6(\mathbb{S},\mathbb{E},\mathbb{I},\mathbb{C},\mathbb{T},\mathbb{R},\mathbb{A}) = \psi(1-\gamma_1)\mathbb{E}(t) + \rho(1-\gamma_2)\mathbb{I}(t) + \nu\mathbb{S}(t) + \gamma_3\mathbb{C}(t) + \gamma_4\mathbb{T}(t) - \mu_0\mathbb{R}(t),$$

$$\mathfrak{F}_7(\mathbb{S},\mathbb{E},\mathbb{I},\mathbb{C},\mathbb{T},\mathbb{R},\mathbb{A}) = r(\mathbb{A}(t) - A_0)\left(1 - \frac{\mathbb{A}(t)}{A_{max}}\right).$$

Let Ω denote the region which is given by

$$\Omega = \left\{ (\mathbb{S}(t), \mathbb{E}(t), \mathbb{I}(t), \mathbb{C}(t), \mathbb{T}(t), \mathbb{R}(t), \mathbb{A}(t)) \in \mathbb{R}_+^7 : \mathbb{N}(t) \leq \frac{b}{\mu_0} \right\}$$

and let $\mathbb{U} \subseteq \Omega$ represent the region $|t - t_0| \leq \delta$, $||x - x_0|| \leq \varepsilon$, where $x = (x_1, x_2, ..., x_n)$ and $x_0 = (x_{1_0}, x_{2_0}, ...x_{n_0})$ also suppose that $a(t, x)$ satisfies the Lipchitz condition:

$$||a(t, x_1) - a(t, x_2)|| \leq k||x_1 - x_2||$$

whenever the pairs (t, x_1), (t, x_2) belongs to $\mathbb{U} \subseteq \Omega$ where k is a positive constant, then there exist a positive constant $\delta \geq 0$, such that there exists a unique and continuous vector solution $x(t)$ of the system (1) in interval $|t - t_0| < \delta$. This condition is satisfied, if $\frac{\partial \mathfrak{F}_i}{\partial x_j} \quad \forall \quad i, j$ are bounded in $\mathbb{U} \subseteq \Omega$, where $x_1 = \mathbb{S}$, $x_2 = \mathbb{E}$, $x_3 = \mathbb{I}$, $x_4 = \mathbb{C}$, $x_5 = \mathbb{T}$, $x_6 = \mathbb{R}$, $x_7 = \mathbb{A}$.

For $\mathfrak{F}_1$;

$$\left|\frac{\partial \mathfrak{F}_1}{\partial \mathbb{S}}\right| = \left|-\frac{\beta(\mathbb{A})\mathbb{I}(t)}{1 + \alpha_2 \mathbb{I}(t)} - (\nu + \mu_0)\right| < \infty, \qquad \left|\frac{\partial \mathfrak{F}_1}{\partial \mathbb{E}}\right| = 0 < \infty, \qquad \left|\frac{\partial \mathfrak{F}_1}{\partial \mathbb{I}}\right| = \left|-\frac{\beta(\mathbb{A})\mathbb{S}(t)}{(1 + \alpha_2 \mathbb{I}(t))^2}\right| < \infty,$$

$$\left|\frac{\partial \mathfrak{F}_1}{\partial \mathbb{C}}\right| = 0 < \infty, \qquad \left|\frac{\partial \mathfrak{F}_1}{\partial \mathbb{T}}\right| = 0 < \infty, \qquad \left|\frac{\partial \mathfrak{F}_1}{\partial \mathbb{R}}\right| = 0 < \infty,$$

$$\left|\frac{\partial \mathfrak{F}_1}{\partial \mathbb{A}}\right| = 0 < \infty$$

The Partial derivative exist, similarly for $\mathfrak{F}_2$, $\mathfrak{F}_3$, $\mathfrak{F}_4$, $\mathfrak{F}_5$, $\mathfrak{F}_6$ and $\mathfrak{F}_7$. This shows that all the partial derivatives $\frac{\partial \mathfrak{F}_i}{\partial x_j} \ \forall \ i, j$ exists, and are continuous as well as bounded in $\mathbb{U} \subseteq \Omega$. This demonstrates that all of the partial derivatives $\frac{\partial \mathfrak{F}_i}{\partial x_j} \ \forall \ i, j$ exist, are continuous and are bounded in $\mathbb{U} \subseteq \Omega$. Hence, by Lipchitz condition, the model (1) has a unique solution. □

3.2 Positivity of the Solution

In this sub-section, we establish positivity of the solutions of model (1) equations.

Theorem 2: *For all given positive initial values, solutions* $\mathbb{S}(t)$, $\mathbb{E}(t)$, $\mathbb{I}(t)$, $\mathbb{C}(t)$, $\mathbb{T}(t)$, $\mathbb{R}(t)$ *and* $\mathbb{A}(t)$ *of system (1) are non-negative* $\forall \ t > 0$.

Proof: Consider first equation of system (1), which implies that,

$$\frac{d\mathbb{S}(t)}{dt} + \left(\frac{\beta(\mathbb{A})\mathbb{I}(t)}{1 + \alpha_2 \mathbb{I}(t)} + (\nu + \mu_0)\right)\mathbb{S}(t) \geq 0, \tag{2}$$

multiplying both sides of inequality (2) by integrating factor and integrating, gives:

$$\mathbb{S}(t) \geq C\, e^{-\left((\nu+\mu_0)t + \int \frac{\beta(\mathbb{A})\mathbb{I}(t)}{1+\alpha_2\mathbb{I}(t)} dt\right)}, \tag{3}$$

where C is a constant of integration. By applying initial condition $\mathbb{S}(0) = \mathbb{S}_0$ and solving gives $C = \mathbb{S}_0$ then substituting in inequality (3), the final solution yields,

$$\mathbb{S}(t) \geq \mathbb{S}_0\, e^{-\left((\nu+\mu_0)t + \int \frac{\beta(\mathbb{A})\mathbb{I}(t)}{1+\alpha_2\mathbb{I}(t)} dt\right)}. \tag{4}$$

In inequality (4), $\mathbb{S}_0 > 0$ and the exponentials are always non-negative. Hence $\mathbb{S}(t) \geq 0, \ \forall \ t > 0$.

The positivity of the remaining state variables $\mathbb{E}(t)$, $\mathbb{I}(t)$, $\mathbb{C}(t)$, $\mathbb{T}(t)$, $\mathbb{R}(t)$ and $\mathbb{A}(t)$ for $t > 0$ can be proved by similar approach. □

3.3 Feasible Region

In this subsection, we establish the boundedness of the state variables and define the feasible region.

Theorem 3 [27]: *The solution for the system (1) is bounded and the closed set* Ω *is biologically feasible region of the system (1) such that* $\Omega = \left\{(\mathbb{S}, \mathbb{E}, \mathbb{I}, \mathbb{C}, \mathbb{T}, \mathbb{R}) \in \mathbb{R}_+^6 : \mathbb{S} > 0, (\mathbb{E}, \mathbb{I}, \mathbb{C}, \mathbb{T}, \mathbb{R}) \geq 0,\ \mathbb{N}(t) \leq \frac{b}{\mu_0}\right\}$.

Proof: Since, the total population is represented by $\mathbb{N}(t)$, where:

$$\mathbb{N}(t) = \mathbb{S}(t) + \mathbb{E}(t) + \mathbb{I}(t) + \mathbb{C}(t) + \mathbb{T}(t) + \mathbb{R}(t), \tag{5}$$

differentiating Eq. (5) *w.r.tt*, substituting the values from system (1) and simplifying, we get:

$$\frac{d\mathbb{N}(t)}{dt} = b - \mu_0 (\mathbb{S} + \mathbb{E} + \mathbb{I} + \mathbb{C} + \mathbb{T} + \mathbb{R}) - \mu_1 \mathbb{I}(t) - \mu_2 \mathbb{C}(t), \tag{6}$$

now, substituting Eq. (5) into Eq. (6), implies that

$$\frac{d\mathbb{N}(t)}{dt} = b - \mu_0 \mathbb{N} - \mu_1 \mathbb{I} - \mu_2 \mathbb{C},$$

this implies that,

$$\frac{d\mathbb{N}(t)}{dt} + \mu_0 \mathbb{N}(t) \leq b, \tag{7}$$

multiplying both sides of inequality (7) by the integrating factor and integrating, we obtain:

$$e^{\mu_0 t}\mathbb{N}(t) \leq \frac{b}{\mu_0} e^{\mu_0 t} + C, \tag{8}$$

where C is a constant of integration. Further, using the initial condition $\mathbb{N}(0) = \mathbb{N}_0$, and solving for C gives $C = \mathbb{N}_0 - \frac{b}{\mu_0}$, then inequality (8) implies that:

$$\mathbb{N}(t) \leq \frac{b}{\mu_0} + \left(\mathbb{N}_0 - \frac{b}{\mu_0}\right) e^{-\mu_0 t}. \tag{9}$$

In inequality (9) when $t \to \infty$, then $\mathbb{N}(t) \to \frac{b}{\mu_0}$ implying that $0 \leq \mathbb{N}(t) \leq \frac{b}{\mu_0}$. As a result, we establish that each solution of system (1) associated with an initial starting point $x_0 \in \mathbb{R}_+^6$ remains in Ω. Hence, the closed region Ω is invariant positively at all times t. Therefore, it is sufficient to examine the dynamics of this model in the region Ω as it is both mathematically well-posed and epidemiologically significant. □

3.4 Equilibrium Points

In this subsection, we calculate two disease-free and disease-endemic equilibrium points when $\mathbb{A}(t) = A_0$ and $\mathbb{A}(t) = A_{max}$.

3.4.1 Disease-Free Equilibrium Point

The disease-free equilibrium point is given by the set $\mathscr{P}^{DFE} = [\mathscr{P}^{DFE}_{A_0}, \mathscr{P}^{DFE}_{A_{max}}]$ such that,

$$\mathscr{P}^{DFE}_{A_0} = (\mathbb{S}^0, \mathbb{E}^0, \mathbb{I}^0, \mathbb{C}^0, \mathbb{T}^0, \mathbb{R}^0, \mathbb{A}^0) = \left(\frac{b}{\nu+\mu_0}, 0, 0, 0, 0, \frac{\nu b}{\mu_0(\nu+\mu_0)}, A_0\right),$$

$$\mathscr{P}^{DFE}_{A_{max}} = (\mathbb{S}^0, \mathbb{E}^0, \mathbb{I}^0, \mathbb{C}^0, \mathbb{T}^0, \mathbb{R}^0, \mathbb{A}^0) = \left(\frac{b}{\nu+\mu_0}, 0, 0, 0, 0, \frac{\nu b}{\mu_0(\nu+\mu_0)}, A_{max}\right).$$

3.4.2 Disease-Endemic Equilibrium Point

The disease-endemic equilibrium point is given by the set $\mathscr{P}^{DEE} = [\mathscr{P}^{DEE}_{A_0}, \mathscr{P}^{DEE}_{A_{max}}]$ such that,

$$\mathscr{P}^{DEE}_{A_0} = \begin{cases} \mathbb{S}^* &= \dfrac{(\rho+\tau_1+\mu_0+\mu_1)(\psi+\mu_0)+b\alpha_2\psi\gamma_1}{\beta_0 b\psi\gamma_1+\alpha_2\psi\gamma_1(\nu+\mu_0)} \\ \mathbb{E}^* &= \dfrac{\beta_0 b\psi\gamma_1-(\rho+\tau_1+\mu_0+\mu_1)(\psi+\mu_0)(\nu+\mu_0)}{(\psi+\mu_0)\psi\gamma_1(\beta_0+(\nu+\mu_0)\alpha_2)} \\ \mathbb{I}^* &= \dfrac{\beta_0 b\psi\gamma_1-(\rho+\tau_1+\mu_0+\mu_1)(\psi+\mu_0)(\nu+\mu_0)}{(\rho+\tau_1+\mu_0+\mu_1)(\psi+\mu_0)(\beta_0+(\nu+\mu_0)\alpha_2)} \\ \mathbb{C}^* &= \dfrac{\rho\gamma_2(\beta_0 b\psi\gamma_1-(\rho+\tau_1+\mu_0+\mu_1)(\psi+\mu_0)(\nu+\mu_0))}{(\rho+\tau_1+\mu_0+\mu_1)(\psi+\mu_0)(\beta_0+(\nu+\mu_0)\alpha_2)(\tau_2+\gamma_3+\mu_0+\mu_2)} \\ \mathbb{T}^* &= \dfrac{(\beta_0 b\psi\gamma_1-(\rho+\tau_1+\mu_0+\mu_1)(\nu+\mu_0)(\psi+\mu_0))(\tau_1(\tau_2+\gamma_3+\mu_0+\mu_2)-\tau_2\rho\gamma_2)}{(\rho+\tau_1+\mu_0+\mu_1)(\tau_2+\gamma_3+\mu_0+\mu_2)(\psi+\mu_0)(\gamma_4+\mu_0)(\beta_0+(\nu+\mu_0)\alpha_2)} \\ \mathbb{R}^* &= \dfrac{\psi(1-\gamma_1)\mathbb{E}^*+\rho(1-\gamma_2)\mathbb{I}^*+\nu\mathbb{S}^*+\gamma_3\mathbb{C}^*+\gamma_4\mathbb{T}^*}{\mu_0} \end{cases} \tag{10}$$

where $\beta(A_0) = \beta_0$, and

$$\mathscr{P}^{DEE}_{A_{max}} = \begin{cases} \mathbb{S}^* &= \dfrac{(\rho+\tau_1+\mu_0+\mu_1)(\psi+\mu_0)+b\alpha_2\psi\gamma_1}{(\beta_0+z\beta_1)b\psi\gamma_1+\alpha_2\psi\gamma_1(\nu+\mu_0)} \\ \mathbb{E}^* &= \dfrac{(\beta_0+z\beta_1)b\psi\gamma_1-(\rho+\tau_1+\mu_0+\mu_1)(\psi+\mu_0)(\nu+\mu_0)}{(\psi+\mu_0)\psi\gamma_1((\beta_0+z\beta_1)+(\nu+\mu_0)\alpha_2)} \\ \mathbb{I}^* &= \dfrac{(\beta_0+z\beta_1)b\psi\gamma_1-(\rho+\tau_1+\mu_0+\mu_1)(\psi+\mu_0)(\nu+\mu_0)}{(\rho+\tau_1+\mu_0+\mu_1)(\psi+\mu_0)((\beta_0+z\beta_1)+(\nu+\mu_0)\alpha_2)} \\ \mathbb{C}^* &= \dfrac{\rho\gamma_2((\beta_0+z\beta_1)b\psi\gamma_1-(\rho+\tau_1+\mu_0+\mu_1)(\psi+\mu_0)(\nu+\mu_0))}{(\rho+\tau_1+\mu_0+\mu_1)(\psi+\mu_0)((\beta_0+z\beta_1)+(\nu+\mu_0)\alpha_2)(\tau_2+\gamma_3+\mu_0+\mu_2)} \\ \mathbb{T}^* &= \dfrac{((\beta_0+z\beta_1)b\psi\gamma_1-(\rho+\tau_1+\mu_0+\mu_1)(\nu+\mu_0)(\psi+\mu_0))(\tau_1(\tau_2+\gamma_3+\mu_0+\mu_2)-\tau_2\rho\gamma_2)}{(\rho+\tau_1+\mu_0+\mu_1)(\tau_2+\gamma_3+\mu_0+\mu_2)(\psi+\mu_0)(\gamma_4+\mu_0)((\beta_0+z\beta_1)+(\nu+\mu_0)\alpha_2)} \\ \mathbb{R}^* &= \dfrac{\psi(1-\gamma_1)\mathbb{E}^*+\rho(1-\gamma_2)\mathbb{I}^*+\nu\mathbb{S}^*+\gamma_3\mathbb{C}^*+\gamma_4\mathbb{T}^*}{\mu_0} \end{cases} \tag{11}$$

where, $\beta(A_{max}) = (\beta_0 + z\beta_1)$ and $z = 1 - \frac{A_0}{A_{max}}$.

3.5 The Basic Reproductive Number $\mathscr{R}_0$

The fundamental reproductive number, $\mathscr{R}_0$, represents the number of secondary infections caused by an infected individual in an entirely vulnerable population. To obtain the basic reproductive number $\mathscr{R}_0$ for model (1), the work of Watmough and Driessche [28] is being followed; accordingly, the non-infected and infected classes must be separated. From model (1), we take the infected classes $\mathbb{E}(t), \mathbb{I}(t), \mathbb{C}(t)$ and $\mathbb{T}(t)$ and let $\mathscr{X} = (\mathbb{E}(t), \mathbb{I}(t), \mathbb{C}(t), \mathbb{T}(t))$, we have,

$$\frac{d\mathscr{X}}{dt} = \mathscr{F} - \mathscr{V}$$

the Jacobian matrices of $\mathscr{F}$ and $\mathscr{V}$ evaluated at the disease-free equilibrium point are,

$$\mathscr{F}^* = \begin{pmatrix} 0 & \beta(\mathbb{A})\mathbb{S}^0 & 0 & 0 \\ 0 & 0 & 0 & 0 \\ 0 & 0 & 0 & 0 \\ 0 & 0 & 0 & 0 \end{pmatrix} \quad \text{and} \quad \mathscr{V}^* = \begin{pmatrix} \psi + \mu_0 & 0 & 0 & 0 \\ -\psi\gamma_1 & \rho + \tau_1 + \mu_0 + \mu_1 & 0 & 0 \\ 0 & -\rho\gamma_2 & \tau_2 + \gamma_3 + \mu_0 + \mu_2 & 0 \\ 0 & -\tau_1 & -\tau_2 & \gamma_4 + \mu_0 \end{pmatrix},$$

the next-generation matrix is given by,

$$\mathscr{F}^*.\mathscr{V}^{*-1} = \begin{pmatrix} \frac{\beta(\mathbb{A})\psi\gamma_1\mathbb{S}^0}{Z_1Z_2} & \frac{\beta(\mathbb{A})\mathbb{S}^0}{Z_2} & 0 & 0 \\ 0 & 0 & 0 & 0 \\ 0 & 0 & 0 & 0 \\ 0 & 0 & 0 & 0 \end{pmatrix},$$

where $Z_1 = \psi + \mu_0$ and $Z_2 = \rho + \tau_1 + \mu_0 + \mu_1$.

The basic reproductive number $\mathscr{R}_0$ is determined as the maximum eigenvalue (the spectral radius, see [29]) of the matrix $\mathscr{F}^*.\mathscr{V}^{*-1}$. Hence,

$$\mathscr{R}_0 = \frac{\beta(\mathbb{A})b\psi\gamma_1}{(\psi + \mu_0)(\nu + \mu_0)(\rho + \tau_1 + \mu_0 + \mu_1)}. \tag{12}$$

From Eq. (12), two different expressions are calculated for $\mathscr{R}_0$. We put $\mathbb{A}(t) = A_0$ in Eq. (12) to compute the first basic reproduction number denoted by $\mathscr{R}_{A_0}$. That is, when a patient with chronic hepatitis B infection consumes even a minimal amount of alcohol, thus,

$$\mathscr{R}_{A_0} = \frac{\beta_0 b\psi\gamma_1}{(\psi + \mu_0)(\nu + \mu_0)(\rho + \tau_1 + \mu_0 + \mu_1)}, \tag{13}$$

by substituting $\mathbb{A}(t) = A_{max}$ in Eq. (12), we compute the other basic reproductive number denoted by $\mathscr{R}_{A_{max}}$. That is, when a patient with chronic hepatitis B infection ingests the maximum amount of alcohol, thus,

$$\mathscr{R}_{A_{max}} = \frac{(\beta_0 + z\beta_1)b\psi\gamma_1}{(\psi + \mu_0)(\nu + \mu_0)(\rho + \tau_1 + \mu_0 + \mu_1)}, \tag{14}$$

assuming $z = 1 - \frac{A_0}{A_{max}}$. We can write $\mathscr{R}_0 = [\mathscr{R}_{A_0}, \mathscr{R}_{A_{max}}]$ in compact form by observing that $0 < \mathscr{R}_{A_0} < \mathscr{R}_{A_{max}}$.

3.6 3D-Type Simulation of $\mathscr{R}_0$

Fig. 2 shows the effect of different model parameters on $\mathscr{R}_{A_0}$ and $\mathscr{R}_{A_{max}}$, respectively.

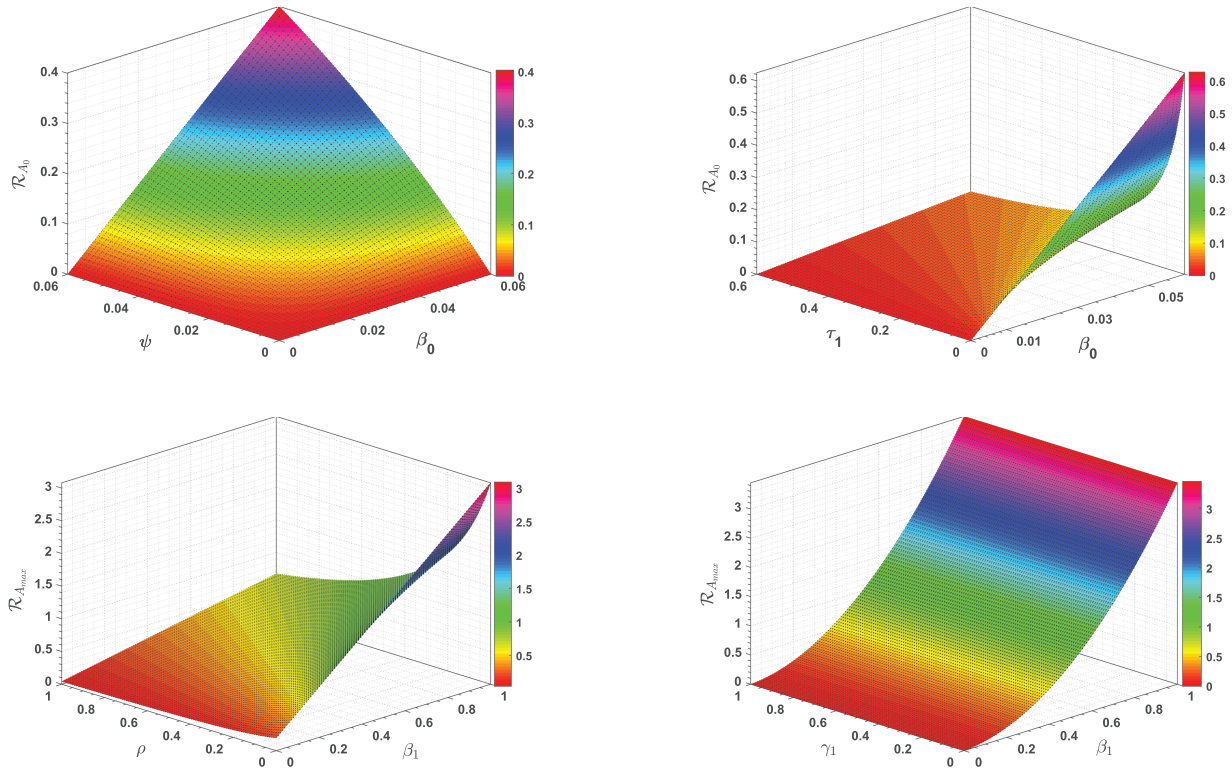

Figure 2: 3D type simulation of $\mathscr{R}_{A_0}$ and $\mathscr{R}_{A_{max}}$

3.7 Stability Analysis

In this subsection, we present both local and global asymptotic stabilities of the equilibria of system (1).

3.7.1 Local Stability

Theorem 4: *The disease-free equilibrium (DFE) point* $\mathscr{P}^{DFE} = [\mathscr{P}^{DFE}_{A_0}, \mathscr{P}^{DFE}_{A_{max}}]$ *is locally asymptotically stable (LAS) when* $\mathscr{R}_{A_0} < \mathscr{R}_{A_{max}} < 1$, *otherwise unstable.*

Proof: The Jacobian matrix of system (1), at disease-free equilibrium point $\mathscr{P}^{DFE}$ when $\mathbb{A}^* \in [A_0, A_{max}]$ is represented by $J(\mathscr{P}^{DFE})$ and given as:

$$J(\mathscr{P}^{DFE}) = \begin{pmatrix} -Z_0 & 0 & -\beta(\mathbb{A}^*)\mathbb{S}^0 & 0 & 0 & 0 & 0 \\ 0 & -Z_1 & \beta(\mathbb{A}^*)\mathbb{S}^0 & 0 & 0 & 0 & 0 \\ 0 & \psi\gamma_1 & -Z_2 & 0 & 0 & 0 & 0 \\ 0 & 0 & \rho\gamma_2 & -Z_3 & 0 & 0 & 0 \\ 0 & 0 & \tau_1 & \tau_2 & -Z_4 & 0 & 0 \\ \nu & Z_5 & Z_6 & \gamma_3 & \gamma_4 & -\mu_0 & 0 \\ 0 & 0 & 0 & 0 & 0 & 0 & -\mathfrak{Z} \end{pmatrix}$$

where,

$$Z_0 = \nu + \mu_0, \quad Z_1 = \psi + \mu_0, \quad Z_2 = \rho + \tau_1 + \mu_0 + \mu_1, \quad Z_3 = \tau_2 + \gamma_3 + \mu_0 + \mu_2,$$

$$Z_4 = \gamma_4 + \mu_0, \quad Z_5 = \psi(1-\gamma_1), \quad Z_6 = \rho(1-\gamma_2), \quad \mathfrak{Z} = \frac{r\,(2\mathbb{A}^* - (A_0 + A_{\max}))}{A_{\max}}.$$

The matrix $J(\mathscr{P}^{DFE})$ can be written in terms of block matrices as,

$$J(\mathscr{P}^{DFE}) = \begin{pmatrix} \mathcal{D}_1 & \mathcal{O} \\ \mathcal{D}_2 & \mathcal{D}_3 \end{pmatrix}$$

where, $\mathcal{O}_{3\times 4}$ is a void matrix and,

$$\mathcal{D}_1 = \begin{pmatrix} -Z_0 & 0 & -\beta^*(\mathbb{A}^*)\mathbb{S}^0 \\ 0 & -Z_1 & \beta^*(\mathbb{A}^*)\mathbb{S}^0 \\ 0 & \psi\gamma_1 & -Z_2 \end{pmatrix}, \qquad \mathcal{D}_2 = \begin{pmatrix} 0 & 0 & \rho\gamma_2 \\ 0 & 0 & \tau_1 \\ \nu & Z_5 & Z_6 \\ 0 & 0 & 0 \end{pmatrix}, \qquad \mathcal{D}_3 = \begin{pmatrix} -Z_3 & 0 & 0 & 0 \\ \tau_2 & -Z_4 & 0 & 0 \\ \gamma_3 & \gamma_4 & -\mu_0 & 0 \\ 0 & 0 & 0 & -\mathfrak{Z} \end{pmatrix},$$

hence, the matrix $J(\mathscr{P}^{DFE})$ is a block diagonal matrix, and thus its eigenvalues are given by:

$\{\text{Eigenvalues of } \mathcal{D}_1\} \cup \{\text{Eigenvalues of } \mathcal{D}_3\}$.

For matrix $\mathcal{D}_3$, the eigenvalues are obtained as, $\lambda_{1,2,3,4} = -Z_3,\ -Z_4,\ -\mu_0,\ -\mathfrak{Z}$ while, matrix $\mathcal{D}_1$ has eigenvalues with negative real parts iff its trace is negative and its determinant is positive [30]. Obviously,

$$\text{Tr } \mathscr{D}_1 = -Z_0 - Z_1 - Z_2 \quad \Rightarrow \text{Tr } \mathscr{D}_1 < 0.$$

Now, to verify that the determinant must be positive, we have

$$|\mathcal{D}_1| = \begin{vmatrix} -Z_0 & 0 & -\beta^*(\mathbb{A}^*)\mathbb{S}^0 \\ 0 & -Z_1 & \beta^*(\mathbb{A}^*)\mathbb{S}^0 \\ 0 & \psi\gamma_1 & -Z_2 \end{vmatrix} > 0,$$

expanding by column 1 and simplifying yields,

$$\frac{\psi\gamma_1\beta(\mathbb{A}^*)\mathbb{S}^0}{Z_1Z_2} < 1,$$

$$\mathscr{R}_0 < 1.$$

Thus, $det(\mathscr{D}_1) > 0 iff \mathscr{R}_0 < 1$. Therefore, this implies that the disease-free equilibrium point $\mathscr{P}^{DFE}$ is locally asymptotically stable when $\mathscr{R}_{A_0} < \mathscr{R}_{A_{max}} < 1$, otherwise unstable. □

Theorem 5: *The disease-endemic equilibrium point* $\mathscr{P}^{DEE} = [\mathscr{P}^{DEE}_{A_0}, \mathscr{P}^{DEE}_{A_{max}}]$ *is locally asymptotically stable when* $\mathscr{R}_{A_{max}} > \mathscr{R}_{A_0} > 1$, *otherwise unstable.*

Proof: The Jacobian matrix of system (1), at disease-endemic equilibrium point $\mathscr{P}^{DEE}$ is represented by $J(\mathscr{P}^{DEE})$ and given as,

$$J(\mathscr{P}^{DEE}) = \begin{pmatrix} -Q_0 & 0 & -Q_1 & 0 & 0 & 0 & 0 \\ Q_2 & -Z_1 & Q_1 & 0 & 0 & 0 & 0 \\ 0 & \psi\gamma_1 & -Z_2 & 0 & 0 & 0 & 0 \\ 0 & 0 & \rho\gamma_2 & -Z_3 & 0 & 0 & 0 \\ 0 & 0 & \tau_1 & \tau_2 & -Z_4 & 0 & 0 \\ \nu & Z_5 & Z_6 & \gamma_3 & \gamma_4 & -\mu_0 & 0 \\ 0 & 0 & 0 & 0 & 0 & 0 & -\mathfrak{Z} \end{pmatrix}$$

where,

$$Q_0 = \frac{\beta(\mathbb{A})\mathbb{I}^*}{1+\alpha_2\mathbb{I}^*} + (\nu+\mu_0), \qquad Q_1 = \frac{\beta(\mathbb{A})\mathbb{S}^*}{(1+\alpha_2\mathbb{I}^*)^2}, \qquad Q_2 = \frac{\beta(\mathbb{A})\mathbb{I}^*}{1+\alpha_2\mathbb{I}^*}$$

$$Z_1 = \psi+\mu_0, \qquad Z_2 = \rho+\tau_1+\mu_0+\mu_1, \qquad Z_3 = \tau_2+\gamma_3+\mu_0+\mu_2,$$

$$Z_4 = \gamma_4+\mu_0, \qquad \mathfrak{Z} = \frac{r\,(2\mathbb{A}^* - (A_0 + A_{\max}))}{A_{\max}},$$

since, the eigenvalues of the Jacobian matrix $J(\mathscr{P}^{DEE})$ are obtained by $|J(\mathscr{P}^{DEE}) - \lambda I| = 0$. Therefore, the four eigenvalues are $\lambda_{1,2,3,4} = -\mathfrak{Z},\ -\mu_0,\ -Z_4,\ -Z_3$ and the remaining are eigenvalues of the following matrix:

$$\mathscr{B} = \begin{pmatrix} -Q_0 & 0 & -Q_1 \\ Q_2 & -Z_1 & Q_1 \\ 0 & \psi\gamma_1 & -Z_2 \end{pmatrix},$$

using the characteristics equation $|\mathscr{B} - \lambda I| = 0$, solving we get the following characteristics polynomial:

$$\lambda^3 + (Q_0+Z_1+Z_2)\lambda^2 + (Q_0Z_1 + Q_0Z_2 + Z_1Z_2 - Q_1\psi\gamma_1)\lambda + Q_0Z_1Z_2 + Q_1\psi\gamma_1(Q_2-Q_0) = 0,$$

this implies that, $f_0\lambda^3 + f_1\lambda^2 + f_2\lambda + f_3 = 0$, where,
$f_0 = 1, \quad f_1 = Q_0+Z_1+Z_2, \quad f_2 = Q_0Z_1 + Q_0Z_2 + Z_1Z_2 - Q_1\psi\gamma_1, \quad f_3 = Q_0Z_1Z_2 + Q_1\psi\gamma_1(Q_2-Q_0)$

Now, we need to verify the following two conditions:

(a) $f_1, f_2, f_3 > 0$ (b) $f_1f_2 - f_0f_3 > 0$

Condition (a) is satisfied as $f_1 > 0$ and $f_2, f_3 > 0\ iff\ Q_0(Z_1+Z_2) + Z_1Z_2 > Q_1\psi\gamma_1\ Q_1 > Q_2$, respectively. Also condition (b) holds if and only if $f_1f_2 > f_0f_3$.

Thus, the Routh-Hurwitz criterion [31] as well as conditions (a) and (b) imply that the characteristic equation has all roots with negative real parts. Thus $\lambda_{5,6,7} < 0$, which guarantees the local stability of disease-endemic equilibrium point $\mathscr{P}^{DEE} = [\mathscr{P}^{DEE}_{A_0}, \mathscr{P}^{DEE}_{A_{max}}]$. □

3.7.2 Global Stability

Theorem 6 [32]: *The disease-free equilibrium point $\mathscr{P}^{DFE} = [\mathscr{P}^{DFE}_{A_0}, \mathscr{P}^{DFE}_{A_{max}}]$, of system (1) is globally asymptotically stable in Ω if $\mathscr{R}_{A_0} < \mathscr{R}_{A_{max}} < 1$.*

Proof: To examine global asymptotic stability of the disease-free equilibrium point of system (1), let us first construct a suitable candidate Lyapunov function $\mathscr{G} : \Delta \subset \mathbb{R}^6_+ \to \mathbb{R}$ where $\Delta = (S, E, I, C)$ such that,

$$\mathscr{G}(S,E,I,C) = \frac{1}{2}\left[(\mathbb{S}(t) - \mathbb{S}^0) + \mathbb{E}(t) + \mathbb{I}(t) + \mathbb{C}(t)\right]^2 \tag{15}$$

clearly, $\mathscr{G} : \Delta \subset \mathbb{R}^6_+ \to \mathbb{R}$ is strictly positive definite and equal to zero at the disease-free equilibrium point $\mathscr{P}^{DFE} = [\mathscr{P}^{DFE}_{A_0}, \mathscr{P}^{DFE}_{A_{max}}]$. Differentiating Eq. (15) with respect to time t, we have,

$$\frac{d\mathscr{G}}{dt} = \left[\left(\mathbb{S}(t) - \mathbb{S}^0\right) + \mathbb{E}(t) + \mathbb{I}(t) + \mathbb{C}(t)\right]\left[\frac{d\mathbb{S}}{dt} + \frac{d\mathbb{E}}{dt} + \frac{d\mathbb{I}}{dt} + \frac{d\mathbb{C}}{dt}\right] \tag{16}$$

substitute values from system (1) to Eq. (16), and simplifying we get,

$$\frac{d\mathscr{G}}{dt} = \left[\left(\mathbb{S}-\mathbb{S}^0\right)+\mathbb{E}+\mathbb{I}+\mathbb{C}\right]\times\Big[b-(\nu+\mu_0)\mathbb{S}-\mu_0\mathbb{E}-\psi\mathbb{E}+\psi\gamma_1\mathbb{E}-\tau_1\mathbb{I}-\mu_1\mathbb{I}-\mu_0\mathbb{I}$$
$$-\rho\mathbb{I}+\rho\gamma_2\mathbb{I}-\tau_2\mathbb{C}-\gamma_3\mathbb{C}-\mu_2\mathbb{C}-\mu_0\mathbb{C}\Big],$$
$$\frac{d\mathscr{G}}{dt} = -\left[\left(\mathbb{S}-\mathbb{S}^0\right)+\mathbb{E}+\mathbb{I}+\mathbb{C}\right]\times\Big[(\nu+\mu_0)\left(\mathbb{S}+\mathbb{S}^0\right)+\mu_0\left(\mathbb{E}+\mathbb{I}+\mathbb{C}+\mathbb{T}\right)+(1-\gamma_1)\psi\mathbb{E}$$
$$+(1-\gamma_2)\rho\mathbb{I}+(\tau_1+\mu_1)\mathbb{I}+(\tau_2+\gamma_3+\mu_2)\mathbb{C}\Big].$$

Thus, $\frac{d\mathscr{G}}{dt} < 0 if \mathscr{R}_{A_0} < \mathscr{R}_{A_{max}} < 1$, and $\frac{d\mathscr{G}}{dt} = 0 iff\ \mathbb{S}(t) = \mathbb{S}^0$ and $\mathbb{E}(t) = \mathbb{I}(t) = \mathbb{C}(t) = 0$. The condition $\mathscr{R}_{A_{max}} < 1$ is the cornerstone for global eradication. It ensures that even under the worst-case scenario of maximum alcohol consumption (A_{max}), which amplifies transmission, the infection cannot sustain itself. When this condition holds, the disease-free state acts as a global attractor, meaning the population will inevitably recover from any initial outbreak and converge to a disease-free state over time. This mathematical guarantee is robust within the model's framework, though its real-world feasibility depends on the system parameters remaining within biologically plausible ranges, as utilized in our numerical simulations.

Hence, the only largest compact positively invariant set is the singleton set $\mathscr{P}^{DFE}$ in $\{(\mathbf{S},\mathbf{E},\mathbf{I},\mathbf{C},\mathbf{T},\mathbf{R}) \in \Omega : (d\mathscr{G}/dt) = 0\}$. □

Theorem 7: *The disease-endemic equilibrium point,* $\mathscr{P}^{DEE} = [\mathscr{P}^{DEE}_{A_0}, \mathscr{P}^{DEE}_{A_{max}}]$, *of system (1) is globally asymptotically stable in* Ω *if* $\mathscr{R}_{A_{max}} > \mathscr{R}_{A_0} > 1$.

Proof: To examine global asymptotic stability of the endemic equilibrium point of system (1), let us first construct a suitable candidate Lyapunov function $\mathscr{F} : \Omega \subset \mathbb{R}^6_+ \to \mathbb{R}$ such that:

$$\mathscr{F}(\mathbb{S},\mathbb{E},\mathbb{I},\mathbb{C},\mathbb{T},\mathbb{R}) = \frac{1}{2}\left(\mathbb{S}-\mathbb{S}^*+\mathbb{E}-\mathbb{E}^*+\mathbb{I}-\mathbb{I}^*+\mathbb{C}-\mathbb{C}^*+\mathbb{T}-\mathbb{T}^*+\mathbb{R}-\mathbb{R}^*\right)^2 \tag{17}$$

clearly, $\mathscr{F} : \mathbb{R}^6_+ \to \mathbb{R}$ is continuously differentiable in $\Omega \subset \mathbb{R}^6_+$ and is strictly positive definite as well as equal to zero at the endemic equilibrium point. Differentiating Eq. (17) with respect to time t, we have,

$$\frac{d\mathscr{F}}{dt} = \left[(\mathbb{N}) - \left(\mathbb{S}^*+\mathbb{E}^*+\mathbb{I}^*+\mathbb{C}^*+\mathbb{T}^*+\mathbb{R}^*\right)\right]\times\left[b-\mu_0\mathbb{N}-\mu_1\mathbb{I}-\mu_2\mathbb{C}\right] \tag{18}$$

where,

$$\mathbb{N} = \mathbb{S}+\mathbb{E}+\mathbb{I}+\mathbb{C}+\mathbb{T}+\mathbb{R}, \quad \text{and} \quad \frac{d\mathbb{N}}{dt} = b-\mu_0\mathbb{N}-\mu_1\mathbb{I}-\mu_2\mathbb{C}.$$

Since,
$b-\mu_0\mathbb{N}^*-\mu_1\mathbb{I}^*-\mu_2\mathbb{C}^* = 0$,
substitute $\mathbb{N}^* = \mathbb{S}^*+\mathbb{E}^*+\mathbb{I}^*+\mathbb{C}^*+\mathbb{T}^*+\mathbb{R}^*$, we have,

$$\left(\mathbb{S}^*+\mathbb{E}^*+\mathbb{I}^*+\mathbb{C}^*+\mathbb{T}^*+\mathbb{R}^*\right) = \frac{b-\mu_1\mathbb{I}^*-\mu_2\mathbb{C}^*}{\mu_0} \tag{19}$$

substitute Eq. (19) in Eq. (18), we get,

$$\begin{aligned}\frac{d\mathscr{F}}{dt} &= \left[\mathbb{N}(t) - \left(\frac{b-\mu_1\mathbb{I}^*-\mu_2\mathbb{C}^*}{\mu_0}\right)\right]\left[b-\mu_0\mathbb{N}-\mu_1\mathbb{I}-\mu_2\mathbb{C}\right],\\ &= -\mu_0\left[\mathbb{N}(t) - \frac{b}{\mu_0} + \frac{\mu_1\mathbb{I}^*+\mu_2\mathbb{C}^*}{\mu_0}\right]\left[\left(\mathbb{N}(t) - \frac{b}{\mu_0} + \frac{\mu_1\mathbb{I}+\mu_2\mathbb{C}}{\mu_0}\right)\right],\\ &\leq -\mu_0\left[\mathbb{N}(t) - \frac{b}{\mu_0}\right]\left[\mathbb{N}(t) - \frac{b}{\mu_0}\right] = -\mu_0\left[\mathbb{N}(t) - \frac{b}{\mu_0}\right]^2.\end{aligned}$$

Thus, $\frac{d\mathscr{F}}{dt} < 0$ if $\mathscr{R}_{A_{max}} > \mathscr{R}_{A_0} > 1$ and $\frac{d\mathscr{F}}{dt} = 0 iff \mathbb{S} = \mathbb{S}^*, \mathbb{E} = \mathbb{E}^*, \mathbb{I} = \mathbb{I}^*, \mathbb{C} = \mathbb{C}^*, \mathbb{T} = \mathbb{T}^*$ and $\mathbb{R} = \mathbb{R}^*$. Hence, the only largest compact positively invariant set in $\{(\mathbb{S}, \mathbb{E}, \mathbb{I}, \mathbb{C}, \mathbb{T}, \mathbb{R}) \in \Omega : (d\mathscr{F}/dt) = 0\}$ is the singleton set $\mathscr{P}^{DEE}$. Therefore, by Lyapunov's asymptotic stability theorem and LaSalle's invariance principle [33], the endemic equilibrium point is globally asymptotically stable in the biologically feasible region Ω if $\mathscr{R}_{A_{max}} > \mathscr{R}_{A_0} > 1$. □

4 Bifurcation Analysis

In this section, we perform the existence of bifurcation, and a detailed proof of forward bifurcation is presented by utilizing the central manifold theory [34] and the method of Chavez & Song [35]. Our proposed model exhibits the same type of bifurcation at $\mathscr{R}_{A_0} = 1$ and $\mathscr{R}_{A_{max}} = 1$.

Existence of Bifurcation

Let us denote $\mathbb{S}(t) = \mathfrak{g}_1, \mathbb{E}(t) = \mathfrak{g}_2, \mathbb{I}(t) = \mathfrak{g}_3, \mathbb{C}(t) = \mathfrak{g}_4, \mathbb{T}(t) = \mathfrak{g}_5, \mathbb{R}(t) = \mathfrak{g}_6$ and $\mathbb{A}(t) = \mathfrak{g}_7$. Thus, in vector notation it becomes $\vec{\mathfrak{g}} = (\mathfrak{g}_1, \mathfrak{g}_2, \mathfrak{g}_3, \mathfrak{g}_4, \mathfrak{g}_5, \mathfrak{g}_6, \mathfrak{g}_7)$ and

$$\frac{d\mathbb{S}(t)}{dt} = y_1(\mathfrak{g}), \quad \frac{d\mathbb{E}(t)}{dt} = y_2(\mathfrak{g}), \quad \frac{d\mathbb{I}(t)}{dt} = y_3(\mathfrak{g}), \quad \frac{d\mathbb{C}(t)}{dt} = y_4(\mathfrak{g})$$
$$\frac{d\mathbb{T}(t)}{dt} = y_5(\mathfrak{g}), \quad \frac{d\mathbb{R}(t)}{dt} = y_6(\mathfrak{g}), \quad \frac{d\mathbb{A}(t)}{dt} = y_7(\mathfrak{g}),$$

thus, system (1) becomes,

$$\begin{cases} y_1(\mathfrak{g}) &= b - \frac{\beta(\mathbb{A}^*)\mathfrak{g}_1\mathfrak{g}_3}{1+\alpha_2\mathfrak{g}_3} - (\nu+\mu_0)\mathfrak{g}_1,\\ y_2(\mathfrak{g}) &= \frac{\beta(\mathbb{A}^*)\mathfrak{g}_1\mathfrak{g}_3}{1+\alpha_2\mathfrak{g}_3} - (\psi+\mu_0)\mathfrak{g}_2,\\ y_3(\mathfrak{g}) &= \psi\gamma_1\mathfrak{g}_2 - (\rho+\tau_1+\mu_0+\mu_1)\mathfrak{g}_3,\\ y_4(\mathfrak{g}) &= \rho\gamma_2\mathfrak{g}_3 - (\tau_2+\gamma_3+\mu_0+\mu_2)\mathfrak{g}_4,\\ y_5(\mathfrak{g}) &= \tau_1\mathfrak{g}_3 + \tau_2\mathfrak{g}_4 - (\gamma_4+\mu_0)\mathfrak{g}_5,\\ y_6(\mathfrak{g}) &= \psi(1-\gamma_1)\mathfrak{g}_2 + \rho(1-\gamma_2)\mathfrak{g}_3 + \nu\mathfrak{g}_1 + \gamma_3\mathfrak{g}_4 + \gamma_4\mathfrak{g}_5 - \mu_0\mathfrak{g}_6,\\ y_7(\mathfrak{g}) &= r(\mathfrak{g}_7 - A_0)\left(1 - \frac{\mathfrak{g}_7}{A_{max}}\right), \end{cases} \tag{20}$$

where $\mathbb{A}^* = [A_0, A_{max}]$.

Let, $y_i (i = 1, ..., 7)$ be a continuous twice differentiable function defined on $\mathbb{R}^7 \times \mathbb{R}$. Thus, Eq. (20) can be written in dynamical system form as;

$$\frac{d\vec{g}}{dt} = y_i(\vec{g}) \tag{21}$$

In Eq. (12), we substitute $\mathscr{R}_0 = 1$ to find the bifurcation parameter $\beta(\mathbb{A}^*)$ and replacing the result by $\beta^*(\mathbb{A}^*)$, which gives:

$$\beta^*(\mathbb{A}^*) = \frac{(\psi+\mu_0)(\nu+\mu_0)(\rho+\tau_1+\mu_0+\mu_1)}{b\psi\gamma_1}$$

The linearization matrix of system (1) evaluated at the disease-free equilibrium point becomes,

$$J^*(\mathscr{P}^{DFE} = \begin{pmatrix} -Z_0 & 0 & -\beta^*(\mathbb{A}^*)\mathbb{S}^0 & 0 & 0 & 0 & 0 \\ 0 & -Z_1 & \beta^*(\mathbb{A}^*)\mathbb{S}^0 & 0 & 0 & 0 & 0 \\ 0 & \psi\gamma_1 & -Z_2 & 0 & 0 & 0 & 0 \\ 0 & 0 & \rho\gamma_2 & -Z_3 & 0 & 0 & 0 \\ 0 & 0 & \tau_1 & \tau_2 & -Z_4 & 0 & 0 \\ \nu & Z_5 & Z_6 & \gamma_3 & \gamma_4 & -\mu_0 & 0 \\ 0 & 0 & 0 & 0 & 0 & 0 & -\mathfrak{Z} \end{pmatrix},$$

The matrix $J^*(\mathscr{P}^{DFE})$ can be written in terms of block matrices as,

$$J^*(\mathscr{P}^{DFE}) = \begin{pmatrix} \mathcal{D}_1 & \mathcal{O} \\ \mathcal{D}_2 & \mathcal{D}_3 \end{pmatrix},$$

where, $\mathcal{O}_{3\times4}$ is null matrix and,

$$\mathcal{D}_1 = \begin{pmatrix} -Z_0 & 0 & -\beta^*(\mathbb{A}^*)\mathbb{S}^0 \\ 0 & -Z_1 & \beta^*(\mathbb{A}^*)\mathbb{S}^0 \\ 0 & \psi\gamma_1 & -Z_2 \end{pmatrix}, \quad \mathcal{D}_2 = \begin{pmatrix} 0 & 0 & \rho\gamma_2 \\ 0 & 0 & \tau_1 \\ \nu & Z_5 & Z_6 \\ 0 & 0 & 0 \end{pmatrix}, \quad \mathcal{D}_3 = \begin{pmatrix} -Z_3 & 0 & 0 & 0 \\ \tau_2 & -Z_4 & 0 & 0 \\ \gamma_3 & \gamma_4 & -\mu_0 & 0 \\ 0 & 0 & 0 & -\mathfrak{Z} \end{pmatrix},$$

hence, the matrix $J^*(\mathscr{P}^{DFE})$ is a block diagonal matrix, and thus its eigenvalues are given by,

$\{\text{Eigenvalues of } \mathcal{D}_1\} \cup \{\text{Eigenvalues of } \mathcal{D}_3\}$.

For matrix $\mathcal{D}_3$, the eigenvalues are obtained through characteristic equation $|\mathcal{D}_3 - \lambda I| = 0$ which are $\lambda_{1,2,3,4} = -Z_3, \ -Z_4, \ -\mu_0, \ -\mathfrak{Z}$ and for the eigenvalues of $\mathcal{D}_1$, we apply the characteristic equation $|\mathcal{D}_1 - \lambda I| = 0$, which yields,

$$|\mathcal{D}_1 - \lambda I| = \begin{vmatrix} -Z_0-\lambda & 0 & -\beta^*(\mathbb{A}^*)S^0 \\ 0 & -Z_1-\lambda & \beta^*(\mathbb{A}^*)S^0 \\ 0 & \psi\gamma_1 & -Z_2-\lambda \end{vmatrix} = 0,$$

this implies that,

$$\lambda^2 + (Z_1+Z_2)\lambda + (1-\mathscr{R}_0) = 0, \tag{22}$$

at $\mathscr{R}_0 = 1$, in Eq. (22) the constant term becomes zero and hence one of the eigenvalues of matrix $\mathcal{D}_1$ must be zero, which guarantees that bifurcation phenomena exist for the system (1).

Theorem 8 [23]**:** *The proposed model (1) exhibits a forward bifurcation at* $\mathscr{R}_0 = 1$ *if* $\mathscr{R}_0 < 1$ *such that* $\mathscr{R}_0 = [\mathscr{R}_{A_0}, \mathscr{R}_{A_{max}}]$.

Proof: We set $\mathscr{R}_0 = 1$ where $\mathscr{R}_0 = [\mathscr{R}_{A_0}, \mathscr{R}_{A_{max}}]$ and calculate the bifurcation parameter β such that $\beta = [\beta_0, \beta_1]$ and consequently replace it with β^* such that $\beta^* = [\beta_0^*, \beta_1^*]$. Thus

$$\beta^* = \frac{(\psi + \mu_0)(\nu + \mu_0)(\rho + \tau_1 + \mu_0 + \mu_1)}{b\psi\gamma_1}.$$

Let us represent the right eigenvectors by $\mathfrak{m} = (\mathfrak{m}_1, \mathfrak{m}_2, \mathfrak{m}_3, \mathfrak{m}_4, \mathfrak{m}_5, \mathfrak{m}_6, \mathfrak{m}_7)^\top$ corresponding to a zero eigenvalue, then

$$J^*(\beta^*).\mathfrak{m} = \begin{pmatrix} -Z_0 & 0 & -\beta^*\mathbb{S}^0 & 0 & 0 & 0 & 0 \\ 0 & -Z_1 & \beta^*\mathbb{S}^0 & 0 & 0 & 0 & 0 \\ 0 & \psi\gamma_1 & -Z_2 & 0 & 0 & 0 & 0 \\ 0 & 0 & \rho\gamma_2 & -Z_3 & 0 & 0 & 0 \\ 0 & 0 & \tau_1 & \tau_2 & -Z_4 & 0 & 0 \\ \nu & Z_5 & Z_6 & \gamma_3 & \gamma_4 & -\mu_0 & 0 \\ 0 & 0 & 0 & 0 & 0 & 0 & -\mathfrak{Z} \end{pmatrix} \begin{pmatrix} \mathfrak{m}_1 \\ \mathfrak{m}_2 \\ \mathfrak{m}_3 \\ \mathfrak{m}_4 \\ \mathfrak{m}_5 \\ \mathfrak{m}_6 \\ \mathfrak{m}_7 \end{pmatrix} = \begin{pmatrix} 0 \\ 0 \\ 0 \\ 0 \\ 0 \\ 0 \\ 0 \end{pmatrix},$$

thus, after simplification, we get the right eigenvectors as follows,

$$\mathfrak{m}_1 = -\frac{\beta^*\mathbb{S}^0\mathfrak{m}_3}{Z_0}, \quad \mathfrak{m}_2 = \frac{\beta^*\mathbb{S}^0\mathfrak{m}_3}{Z_1}, \quad \mathfrak{m}_3 = \frac{\psi\gamma_1\mathfrak{m}_2}{Z_2}, \quad \mathfrak{m}_4 = \frac{\rho\gamma_2\mathfrak{m}_3}{Z_3},$$
$$\mathfrak{m}_5 = \frac{\tau_1\mathfrak{m}_3 + \tau_2\mathfrak{m}_4}{Z_4}, \quad \mathfrak{m}_6 = \frac{\nu\mathfrak{m}_1 + Z_5\mathfrak{m}_2 + Z_6\mathfrak{m}_3 + \gamma_3\mathfrak{m}_4 + \gamma_4\mathfrak{m}_5}{\mu_0}, \quad \mathfrak{m}_7 = 0,$$

similarly, let the left eigenvector is represented by $\mathfrak{v} = (\mathfrak{v}_1, \mathfrak{v}_2, \mathfrak{v}_3, \mathfrak{v}_4, \mathfrak{v}_5, \mathfrak{v}_6, \mathfrak{v}_7)^\top$ corresponding to a zero eigenvalue (i.e., $\lambda = 0$), then,

$$(J^*(\beta^*))^\top.\mathfrak{v} = \begin{pmatrix} -Z_0 & 0 & 0 & 0 & 0 & \nu & 0 \\ 0 & -Z_1 & \psi\gamma_1 & 0 & 0 & Z_5 & 0 \\ -\beta^*\mathbb{S}^0 & \beta^*\mathbb{S}^0 & -Z_2 & \rho\gamma_2 & \tau_1 & Z_6 & 0 \\ 0 & 0 & 0 & -Z_3 & \tau_2 & \gamma_3 & 0 \\ 0 & 0 & 0 & 0 & -Z_4 & \gamma_4 & 0 \\ 0 & 0 & 0 & 0 & 0 & -\mu_0 & 0 \\ 0 & 0 & 0 & 0 & 0 & 0 & -\mathfrak{Z} \end{pmatrix} \begin{pmatrix} \mathfrak{v}_1 \\ \mathfrak{v}_2 \\ \mathfrak{v}_3 \\ \mathfrak{v}_4 \\ \mathfrak{v}_5 \\ \mathfrak{v}_6 \\ \mathfrak{v}_7 \end{pmatrix} = \begin{pmatrix} 0 \\ 0 \\ 0 \\ 0 \\ 0 \\ 0 \\ 0 \end{pmatrix},$$

thus, after simplification, we get the left eigenvectors as follows,

$$\mathfrak{v}_1 = 0, \quad \mathfrak{v}_2 = \frac{\psi\gamma_1\mathfrak{v}_3}{Z_1}, \quad \mathfrak{v}_3 = \frac{\beta^*\mathbb{S}^0\mathfrak{v}_2}{Z_2}, \quad \mathfrak{v}_4 = 0, \quad \mathfrak{v}_5 = 0, \quad \mathfrak{v}_6 = 0, \quad \mathfrak{v}_7 = 0$$

Let, $y_k(k = 1, \ldots, 7)$ be the k^{th} component of $y_i(i = 1, \ldots, 7)$ in Eq. (20) with,

$$a_1 = \sum_{i,j,k=1}^{7} \mathfrak{v}_k\mathfrak{m}_i\mathfrak{m}_j\frac{\partial^2 y_k}{\partial\mathfrak{g}_i\partial\mathfrak{g}_j} \tag{23}$$

$$a_2 = \sum_{j,k=1}^{7} \mathfrak{v}_k\mathfrak{m}_j\frac{\partial^2 y_k}{\partial\mathfrak{g}_j\partial\beta^*} \tag{24}$$

To calculate a_1, we find the non-zero second ordered partial derivatives of $y_k(k = 1, ..., 7)$ with respect to $\mathfrak{g}_i(i = 1, ..., 7)$ and $\mathfrak{g}_j(j = 1, ..., 7)$ around the disease-free equilibrium and to calculate a_2, we find the non-zero second ordered partial derivatives of $y_k(k = 1, ..., 7)$ with respect to $\mathfrak{g}_j(j = 1, ..., 7)$ and β^* around the disease-free equilibrium.

$y_2(\mathfrak{g})$ and $y_3(\mathfrak{g})$ are the only functions at which the components of the left eigenvector $\mathfrak{v}$ are non-zero. Therefore, we calculate their second-order partial derivatives with respect to $\mathfrak{g}_i$ and $\mathfrak{g}_j \forall i, j$.

$$\begin{cases} y_2(\mathfrak{g}) &= \dfrac{\beta^* \mathfrak{g}_1 \mathfrak{g}_3}{1 + \alpha_2 \mathfrak{g}_3} - (\psi + \mu_0)\mathfrak{g}_2, \\ y_3(\mathfrak{g}) &= \psi \gamma_1 \mathfrak{g}_2 - (\rho + \tau_1 + \mu_0 + \mu_1)\mathfrak{g}_3, \end{cases}$$

the second ordered partial derivatives of the function $y_2(\mathfrak{g})$ are given by,

$$\frac{\partial^2 y_2}{\partial \mathfrak{g}_1 \partial \mathfrak{g}_j} = \begin{cases} \beta^*, & for \quad j = 3 \\ 0, & for \quad j \neq 3 \end{cases}, \frac{\partial^2 y_2}{\partial \mathfrak{g}_3 \partial \mathfrak{g}_j} = \begin{cases} \beta^*, & for \quad j = 1 \\ 0, & for \quad j \neq 1 \end{cases}$$

$$\frac{\partial^2 y_2}{\partial \mathfrak{g}_2 \partial \mathfrak{g}_j} = \frac{\partial^2 y_2}{\partial \mathfrak{g}_4 \partial \mathfrak{g}_j} = \frac{\partial^2 y_2}{\partial \mathfrak{g}_5 \partial \mathfrak{g}_j} = \frac{\partial^2 y_2}{\partial \mathfrak{g}_6 \partial \mathfrak{g}_j} = \frac{\partial^2 y_2}{\partial \mathfrak{g}_7 \partial \mathfrak{g}_j} = 0 \quad \text{similarly,} \quad \frac{\partial^2 y_3}{\partial \mathfrak{g}_1 \partial \mathfrak{g}_j} = 0, \quad \forall j$$

the second ordered partial derivatives of $y_2(\mathfrak{g})$ and $y_3(\mathfrak{g})$ with respect to $\mathfrak{g}_j(j = 1, ..., 7)$ and β^* are given by,

$$\frac{\partial^2 y_2}{\partial \mathfrak{g}_j \partial \beta^*} = \begin{cases} \mathbb{S}^0, & for \quad j = 3 \\ 0, & for \quad j \neq 3 \end{cases} \quad \text{similarly,} \quad \frac{\partial^2 y_3}{\partial \mathfrak{g}_j \partial \beta^*} = 0, \quad \forall j.$$

To find a_1, we consider only the non-zero second ordered partial derivatives of $y_2(\mathfrak{g})$ and $y_3(\mathfrak{g})$. Therefore, Eq. (23) becomes

$$a_1 = 2\mathfrak{v}_2 \mathfrak{m}_1 \mathfrak{m}_3 \frac{\partial^2 y_2}{\partial \mathfrak{g}_1 \partial \mathfrak{g}_3}$$

since $\mathfrak{m}_1 < 0$ and all other values are positive, therefore we observe that $a_1 < 0$.

Similarly, considering the non-zero second-order partial derivatives Eq. (24) becomes,

$$a_2 = \frac{\mathfrak{v}_2 S^0 \psi \gamma_1 \mathfrak{m}_2}{Z_2},$$

all values on *RHS* are positive thus, $a_2 > 0$.

When $a_1 < 0$ and $a_2 > 0$, then the bifurcation is forward [36]. In this circumstance, the disease-free equilibrium ceases to be stable, while a stable endemic equilibrium appears as $\mathscr{R}_0$ increases through one. In this case, if $\mathscr{R}_0 < 1$, the system is attracted to the disease-free equilibrium; that is, any small infection will die out. In the case of $\mathscr{R}_0 > 1$, the endemic equilibrium turns out to be stable. □

The forward bifurcation analysis of our model offers profound biological insights into the dynamics of hepatitis B and alcohol-induced liver cirrhosis. As $\mathscr{R}_0$ exceeds one, the system transitions from a disease-free state to an endemic state, marked by the coexistence of a stable endemic equilibrium with the unstable disease-free equilibrium. This transition highlights the critical threshold at which the disease becomes persistent in the population. The absence of backward bifurcation implies that reducing $\mathscr{R}_0$ below one is both necessary and sufficient for disease eradication, emphasizing the efficacy of interventions like vaccination and treatment. These results align with clinical observations, where sustained control measures are essential

to prevent the endemic spread of liver cirrhosis in populations with high hepatitis B prevalence and alcohol consumption. The forward bifurcation thus serves as a mathematical validation of the importance of early and continuous public health efforts to mitigate disease progression.

Furthermore, the forward bifurcation provides a clear biological interpretation of the transition from controlled infection states to endemic persistence. It demonstrates that the disease dynamics are governed by a sharp, predictable threshold at $\mathscr{R}_0 = 1$. When $\mathscr{R}_0 < 1$, the system is attracted to the disease-free equilibrium, indicating that minor outbreaks will fade out independently, representing a controlled state. Once $\mathscr{R}_0$ surpasses this critical value, the system undergoes a qualitative shift to a stable endemic state, where the infection is self-sustaining within the population. This bifurcation structure confirms that there is no reservoir of infection or bistability at sub-threshold values; consequently, pushing the basic reproductive number below unity through targeted interventions is a reliable strategy for disease eradication. This insight reinforces the critical need for public health policies aimed at reducing transmission factors, such as high alcohol consumption in Hepatitis B carriers, to maintain the population below this epidemiological tipping point.

5 Sensitivity Analysis

In this section, we compute the sensitivity indices of the threshold number $\mathscr{R}_0$. Using these indices, we figure out the most influential parameters that are responsible for the disease transmission and control. To perform sensitivity analysis, we use the formula developed by Chitnis et al. [37]. The standard forward sensitivity index of $\mathscr{R}_0$ is given by

$$\mathscr{X}_{\xi}^{\mathscr{R}_0} = \frac{\partial \mathscr{R}_0}{\partial \xi} \times \frac{\xi}{\mathscr{R}_0} \tag{25}$$

where, ξ represents the set of model parameters such that $\xi = \{\beta(A^*), b, \psi, \gamma_1, \mu_0, \nu, \rho, \tau_1, \mu_1\}$.

The sensitivity indices of $\mathscr{R}_0 = [\mathscr{R}_{A_0}, \mathscr{R}_{A_{max}}]$ are calculated using the formula (25) $w.r.t$ the model parameters.

Case-I: The sensitivity indices of $\mathscr{R}_{A_0} w.r.t \xi$ such that $\xi = \{\beta_0, b, \psi, \gamma_1, \mu_0, \nu, \rho, \tau_1, \mu_1\}$ are calculated as,

$$\mathscr{X}_{\mu_0}^{\mathscr{R}_{A_0}} = -\frac{\mu_0\{(\rho+\tau_1+\mu_0+\mu_1)(\nu+\psi+2\mu_0)+(\psi+\mu_0)(\nu+\mu_0)\}}{(\rho+\tau_1+\mu_0+\mu_1)(\psi+\mu_0)(\nu+\mu_0)} = -1.606600$$

and the remaining are listed in Table 2.

Table 2: Sensitivity analysis of model parameters in $\mathscr{R}_{A_0}$ and $\mathscr{R}_{A_{max}}$

Parameter	Value per year	Source	$\mathscr{X}_{\xi}^{\mathscr{R}_{A_0}}$	$\mathscr{X}_{\xi}^{\mathscr{R}_{A_{max}}}$
b	0.5800	[25]	+1.000000	+1.000000
μ_0	0.0300	[8]	−1.606600	−1.606600
μ_1	0.0020	[8]	−0.019608	−0.019608
β_0	0.0050	[8]	+1.000000	+0.362319
β_1	0.0120	[Assumed]	–	+0.637681
ψ	0.0500	[Assumed]	+2.666667	+2.666667
γ_1	0.6000	[Assumed]	+1.000000	+1.000000
ρ	0.0600	[Assumed]	−0.588235	−0.588235
τ_1	0.0100	[Assumed]	−0.098039	−0.098039
ν	0.0020	[25]	−0.062500	−0.062500

Case-II: The sensitivity indices of $\mathscr{R}_{A_{max}} w.r.t \xi$ such that $\xi = \{\beta_0, \beta_1, b, \psi, \gamma_1, \mu_0, \nu, \rho, \tau_1, \mu_1\}$ are calculated using (25) as follows:

$$\mathscr{X}_{\beta_0}^{\mathscr{R}_{A_{max}}} = \frac{\partial \mathscr{R}_{A_{max}}}{\partial \beta_0} \times \frac{\beta_0}{\mathscr{R}_{A_{max}}} = \frac{\beta_0}{\beta_0 + z\beta_1} = +0.362319, \quad \mathscr{X}_{\beta_1}^{\mathscr{R}_{A_{max}}} = \frac{\partial \mathscr{R}_{A_{max}}}{\partial \beta_1} \times \frac{\beta_1}{\mathscr{R}_{A_{max}}} = \frac{z\beta_1}{\beta_0 + z\beta_1} = +0.637681$$

and other are listed in Table 2.

In Table 2, each model parameter's sensitivity index is shown in relation to the fundamental reproduction numbers $\mathscr{R}_{A_0}$ and $\mathscr{R}_{A_{max}}$. In Table 2, some of the parameters are positive, while others are negative. This allows us to provide the biological interpretation of each model parameter in $\mathscr{R}_{A_0}$ and $\mathscr{R}_{A_{max}}$. Positive sign parameters indicates that $\mathscr{R}_{A_0}$ and $\mathscr{R}_{A_{max}}$ are positively impacted by them. Conversely, negative sign parameters affect $\mathscr{R}_{A_0}$ and $\mathscr{R}_{A_{max}}$ negatively. Parameters like β_0, β_1, b, ψ, and γ_1 have positive signs and are directly related to $\mathscr{R}_{A_0}$ and $\mathscr{R}_{A_{max}}$. This biologically means that an increase (or decrease) in the value of the parameter automatically increases (or decreases) $\mathscr{R}_{A_0}$ and $\mathscr{R}_{A_{max}}$. Additionally, the fundamental reproduction numbers are inversely related to parameters with negative signs, such as μ_0, μ_1, ν, ρ, and τ_1. Consequently, the increase in the parameter values is directly responsible for the decrease (respectively increasing) of $\mathscr{R}_{A_0}$ and $\mathscr{R}_{A_{max}}$. We note that the sensitivity indices allow us to find out factors that spread illness and the best ways to prevent it. In Fig. 2, we have visualized the effect of these parameters for $\mathscr{R}_{A_0}$ and $\mathscr{R}_{A_{max}}$ respectively where the most influential parameter is ψ. Increasing the values of ψ and β_0 while keeping other parameters constant will also increase the basic reproduction number $\mathscr{R}_{A_0}$. Furthermore, keeping the values of other parameters fixed and increasing the values of γ_1 and β_1, the basic reproduction number $\mathscr{R}_{A_{max}}$ will also increase. These parameters, therefore, imply that they are directly related to $\mathscr{R}_{A_0}$ and $\mathscr{R}_{A_{max}}$. In Fig. 3, the sensitivity indices of the fundamental model parameters are shown diagrammatically. The results in Fig. 3b shows that the impact of β_1 on $\mathscr{R}_{A_{max}}$ is more than that of β_0 and that β_1 does not influence $\mathscr{R}_{A_0}$ at all.

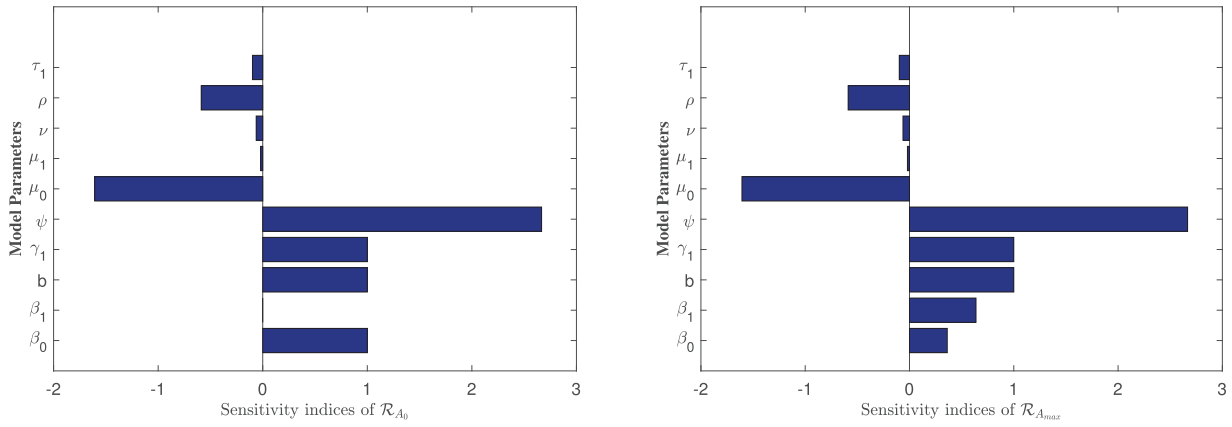

Figure 3: Sensitivity indices of the model parameters in (**a**) $\mathscr{R}_{A_0}$ and (**b**) $\mathscr{R}_{A_{max}}$

The sensitivity analysis of $\mathscr{R}_{A_{\max}}$ is conducted to evaluate the influence of alcohol-dependent parameters, particularly β_0 and β_1, on disease transmission dynamics. The results, presented in Table 2 and Fig. 3b, reveal that β_1 exhibits a stronger effect on $\mathscr{R}_{A_{\max}}$ compared to β_0, emphasizing the non-linear relationship between alcohol consumption and disease spread. This analysis underscores the critical role of alcohol in

exacerbating HBV-induced liver cirrhosis, aligning with our model's focus on the combined effects of alcohol and Hepatitis B infection. The inclusion of these findings ensures a robust examination of all influential parameters, including those specific to alcohol intake.

6 Global Sensitivity Analysis

While local sensitivity analysis provides valuable insights into the effect of infinitesimal parameter changes around a nominal value, it has limitations. Local sensitivity analysis cannot capture the effects of large parameter variations, interactions between parameters, or non-linearities in the model output over the entire feasible parameter space. To address these limitations and test the robustness of our findings to parameter uncertainty, we complement the Local sensitivity analysis with a global, variance-based sensitivity analysis using the Sobol's method.

The Sobol' method decomposes the total variance of the model output (in this case, the basic reproductive number $\mathscr{R}_0$) into fractions attributable to individual parameters and their interactions. It computes two key indices for each parameter ξ_i:

- **First-order index (S_i):** Measures the main effect of ξ_i, representing the fraction of output variance reduced by fixing ξ_i.
- **Total-order index (ST_i):** Measures the total effect of ξ_i, including all variance caused by its interactions (of any order) with all other parameters. The difference $ST_i - S_i$ quantifies the magnitude of these interaction effects.

We performed this analysis for $\mathscr{R}_A^{max}$, as it represents the worst-case transmission scenario. Parameter ranges were defined as ±10% around their nominal values from Table 1, reflecting realistic uncertainty in their estimation. We generated $N = 10,000$ parameter samples using a Sobol sequence to ensure efficient space-filling and computed the Sobol indices.

6.1 Interpretation of Results

The global sensitivity analysis (Table 3 and Fig. 4) largely confirms the ranking of parameter importance identified by the local method (Table 2): the transmission rate from exposed to infected (ψ), the natural death rate (μ_0), and the recruitment rate (b) remain the most influential parameters. This consistency reinforces the robustness of our local findings for small perturbations.

Table 3: Sobol sensitivity indices for model parameters

Parameter	Si	STi
b	0.00527	0.00227
μ_0	0.79233	0.84290
μ_1	0.00473	0.00059
β_0	0.10807	0.10742
β_1	0.00445	0.00010
ψ	0.01614	0.01445
γ_1	0.02859	0.01352
ρ	0.03893	0.01764
τ_1	0.00459	0.00152
ν	0.00875	−0.00064

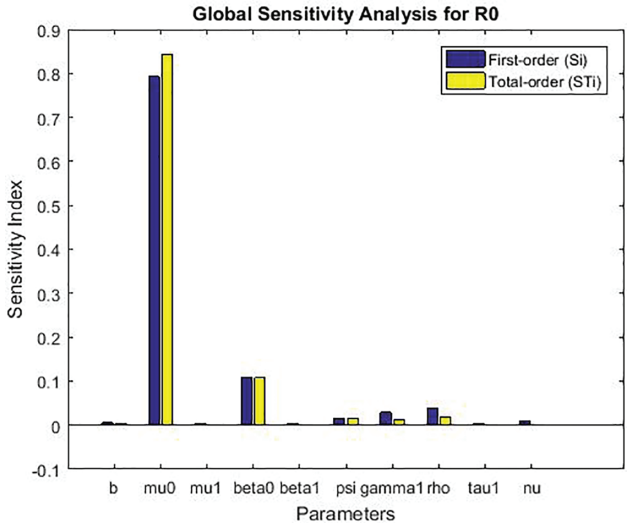

Figure 4: Global sensitivity analysis showing first-order (S_i) and total-order (S_{T_i}) Sobol' indices for the basic reproduction number $\mathscr{R}_0$

However, the Sobol's analysis provides critical additional insights:

- **Interaction Effects:** For several parameters, notably β_1, β_0, and ρ, the total-order index (ST_i) is noticeably larger than the first-order index (S_i). For example, for β_1, $ST_i - S_i = 0.019$. This indicates that a significant portion of this parameter's influence on R_0 is realized through its interactions with other parameters (e.g., with ψ or b). This non-additive effect is clearly visible in Fig. 4 but completely invisible to local analysis.
- **Robustness to Uncertainty:** The analysis confirms that the model's behavior is most sensitive to uncertainty in the parameters ψ and μ_0, as they have the largest absolute indices. This means that public health efforts aimed at reducing ψ (e.g., through improved early diagnosis to shorten the infectious period) and accurate estimation of the baseline mortality rate μ_0 are paramount for reliable model predictions.
- **Refined Prioritization:** While local analysis ranked γ_1 and β_1 similarly, the global analysis shows that the main effect of γ_1 ($S_i = 0.188$) is slightly higher than that of β_1 ($S_i = 0.184$), but the total effect of β_1 ($ST_i = 0.203$) is higher due to its interactions. This nuanced view is crucial for prioritization: controlling the fraction moving to acute infection (γ_1) has a more direct impact, but the effect of alcohol consumption (β_1) is amplified through its interactions within the system.

In conclusion, the global sensitivity analysis validates the primary drivers of the model identified locally while revealing important interaction effects, particularly involving alcohol consumption parameters. It demonstrates that the model's output is robust to the uncertainty in the estimated parameters, as the relative importance remains consistent, and provides a more comprehensive foundation for designing targeted intervention strategies.

6.2 Discussion of Sensitivity Analysis Figures

The sensitivity analysis produces several figures that illustrate the effect of model parameters on the basic reproduction number $\mathscr{R}_0$. In Fig. 5a, scatter plots obtained through Latin Hypercube Sampling (LHS) show the direct relationship between each parameter and $\mathscr{R}_0$. In Fig. 5b, a bar chart of local elasticities highlights the relative sensitivity of $\mathscr{R}_0$ to small perturbations around baseline values. Sobol sensitivity indices are presented using grouped bar plots, distinguishing first-order and total-order effects to capture

both individual and interaction contributions. Finally, Partial Rank Correlation Coefficient (PRCC) values are displayed in bar charts, providing correlation-based rankings of parameter importance. Together, these figures give a clear and complementary view of the relative influence of parameters on $\mathscr{R}_0$.

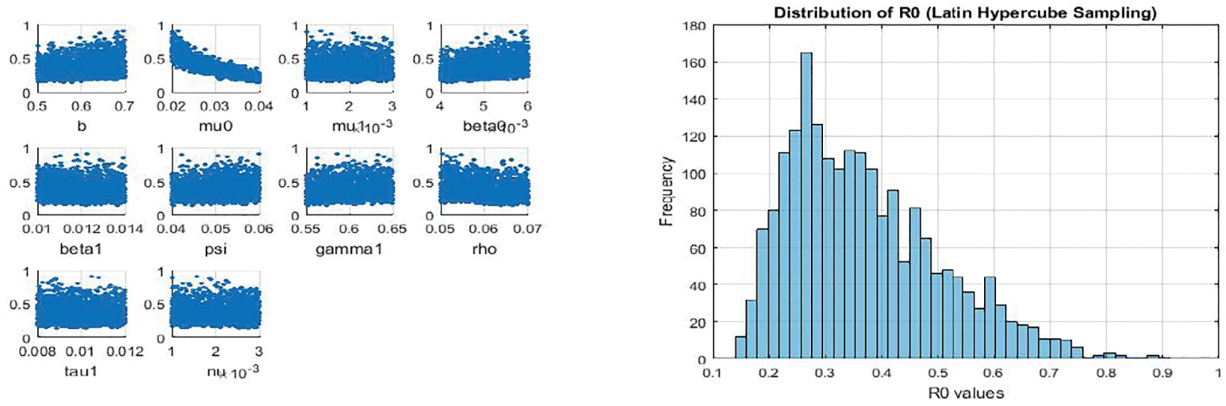

(a) Latin Hypercube Sampling (Scatter Plot)

(b) Latin Hypercube Sampling (Bar Chart)

Figure 5: Comparison of Latin hypercube sampling results

7 Numerical Simulation

In this section, the numerical simulations of the proposed model (1) are carried out by employing MATLAB programming of *ODE*45 solver built-in function and RK-4 method. For the simulation, we used a set of positive initial data 120, 60, 30, 15, 5 and 5 in thousands for the states in Eq. (1), $\mathbb{S}$, $\mathbb{E}$, $\mathbb{I}$, $\mathbb{C}$, $\mathbb{T}$ and $\mathbb{R}$, respectively. We utilized the parameter values in Table 1 and assumed a time interval of 0−200 months. Some of the parameter values are taken from previously published research articles and the other are assumed.

The clinical implications of the reproductive numbers $\mathscr{R}_{A_0}$ and $\mathscr{R}_{A_{max}}$ are profound for understanding liver cirrhosis progression under Hepatitis B and alcohol co-exposure. When both $\mathscr{R}_{A_0} > 1$ and $\mathscr{R}_{A_{max}} > 1$, the disease remains endemic irrespective of alcohol consumption levels, reflecting a high baseline Hepatitis B transmission rate compounded by alcohol's synergistic effect. This scenario demands comprehensive interventions, including universal vaccination, antiviral therapy, and stringent alcohol abstinence programs, to mitigate the accelerated progression to cirrhosis and hepatocellular carcinoma. The dual-threshold exceedance underscores the necessity of integrated public health policies targeting both viral suppression and behavioral modifications.

Conversely, if only $\mathscr{R}_{A_{max}} > 1$ (with $\mathscr{R}_{A_0} \leq 1$), the endemicity is contingent upon high alcohol intake, suggesting that cirrhosis progression can be controlled by reducing alcohol consumption below A_{max}. This outcome highlights the efficacy of targeted alcohol-reduction campaigns and personalized clinical advice for at-risk populations. In scenarios where solely $\mathscr{R}_{A_0} > 1$ (with $\mathscr{R}_{A_{max}} \leq 1$), Hepatitis B transmission dominates, and alcohol plays a negligible role. Here, interventions should prioritize HBV-specific measures such as neonatal vaccination and early treatment, with less urgency for alcohol-related restrictions. These findings emphasize the importance of context-specific strategies, aligning clinical and public health efforts with the dominant drivers of disease progression in each scenario.

In Fig. 6, the curves represent the dynamic behavior of susceptible, exposed, acutely infected, liver cirrhotic, treated, and recovered individuals. Observing the figure, the susceptible population decreases while the exposed, acutely infected, liver cirrhotic, treated, and recovered populations increase for over 80 months and start falling sharply to zero afterward. In both figures, when low and high amounts of alcohol are consumed, all trajectories are converging to $(18.125, 0, 0, 0, 0, 1.208)$, verifying the local stability of the disease-free equilibrium of system (1). Fig. 7 shows the impact of alcohol consumption on the progression dynamics of each compartment. As clearly seen from sub-figure (a), as alcohol consumption increases, the number of susceptible individuals decreases, while from sub-figure (b), the exposed individuals increase significantly. From sub-figures (c) and (d), it can be observed that alcohol use by a Hepatitis B-infected individual accelerates the progression of acute infection and liver cirrhosis, respectively. Fig. 8 shows the simulation results for the variation of the baseline transmission rate β_0. The Increase in this rate results in an increase in the exposed, acutely infected, and liver cirrhotic population. To minimize the transmission rate, alcohol usage incremental rate should be decreased. Fig. 9 shows the simulation results for the variation of parameter ψ which demonstrates that variations in parameter ψ yields a tremendous change in each compartment. It indicates that if all other model parameters are kept fixed and only varying the parameter ψ, the exposed, acutely infected, and liver cirrhotic individuals increase. Fig. 10 shows the simulation results for the variation of parameter ρ, which yields a dramatic increase in the cirrhotic individuals. Consequently, the acutely infected individuals decrease because they are transferring to the cirrhotic class. It indicates that if only varying the parameter ρ and keeping all other fixed, the liver cirrhotic individuals increases. Fig. 11 shows the simulation results for the saturation parameter α_2, which demonstrates that by varying α_2, the susceptible individuals increase while exposed, acutely infected, and cirrhotic individuals decrease.

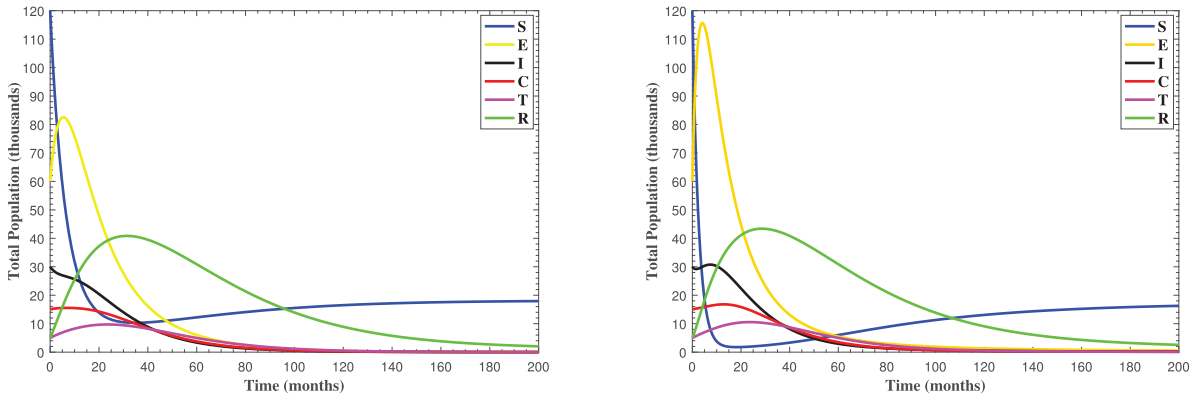

(a) When alcohol consumption is $\mathbb{A}(t) = A_0$ and $\mathscr{R}_{A_0} = 0.333180 < 1$

(b) When alcohol consumption is $\mathbb{A}(t) = A_{max}$ and $\mathscr{R}_{A_{max}} = 0.919577 < 1$

Figure 6: The plots show how all trajectories of the state variables $\mathbb{S}(t)$, $\mathbb{E}(t)$, $\mathbb{I}(t)$, $\mathbb{C}(t)$, $\mathbb{T}(t)$ and $\mathbb{R}(t)$ converge to the disease-free equilibrium

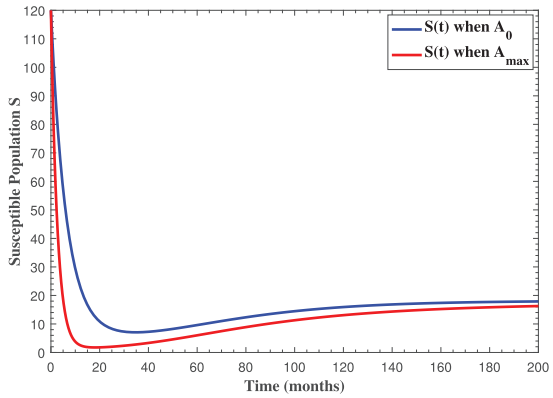

(a) Susceptible Population

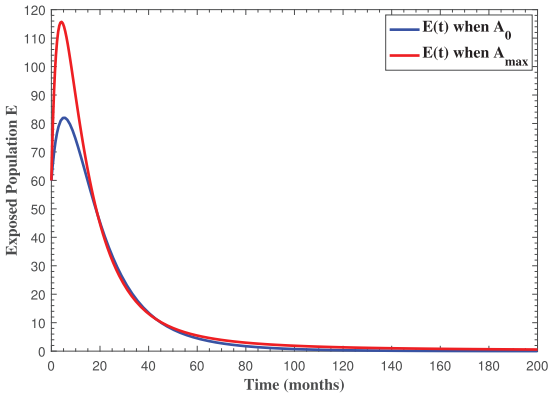

(b) Exposed Population

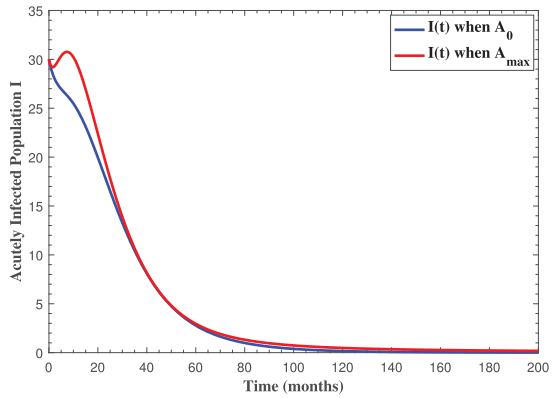

(c) Acutely Infected Population

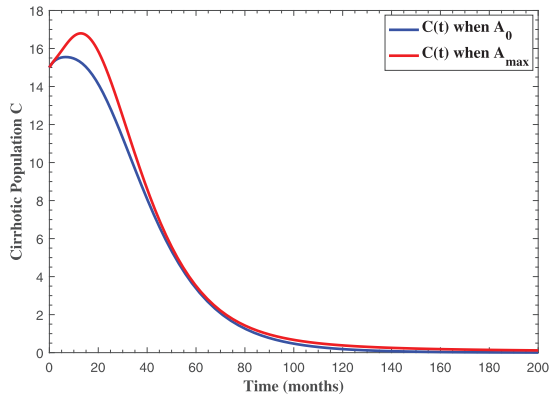

(d) Cirrhotic Population

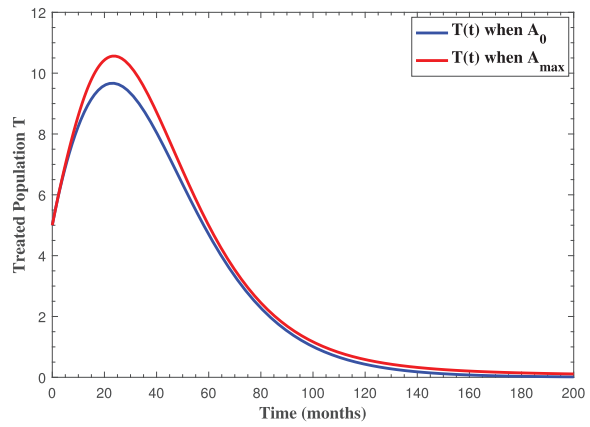

(e) Treated Population

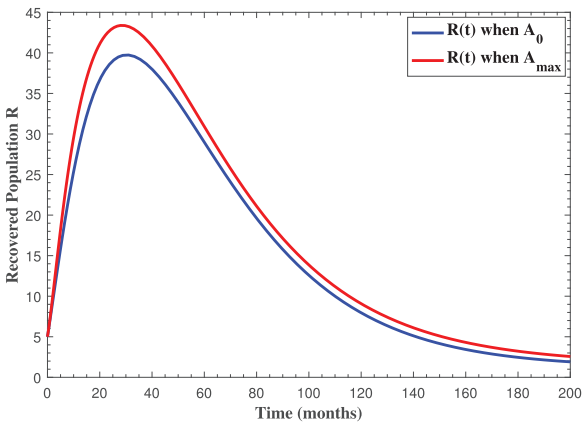

(f) Recovered Population

Figure 7: The graphs show the simulation results of $\mathbb{S}(t)$, $\mathbb{E}(t)$, $\mathbb{I}(t)$, $\mathbb{C}(t)$, $\mathbb{T}(t)$ and $\mathbb{R}(t)$

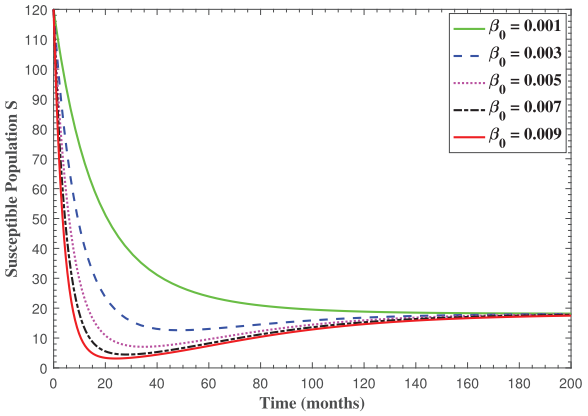

(a) Susceptible Population

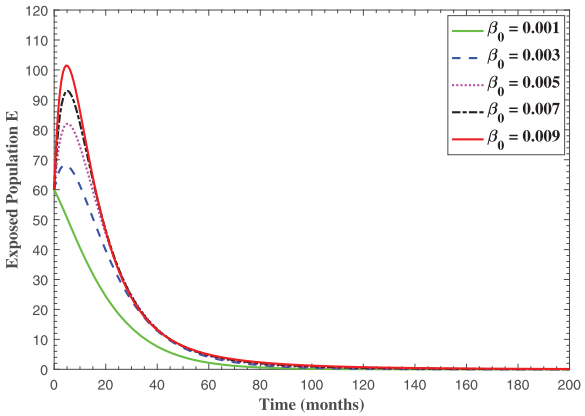

(b) Exposed Population

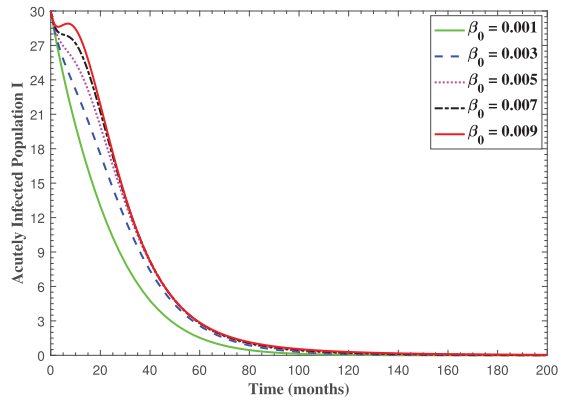

(c) Acutely Infected Population

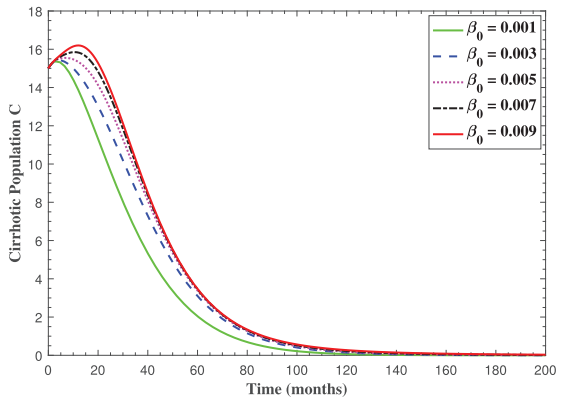

(d) Cirrhotic Population

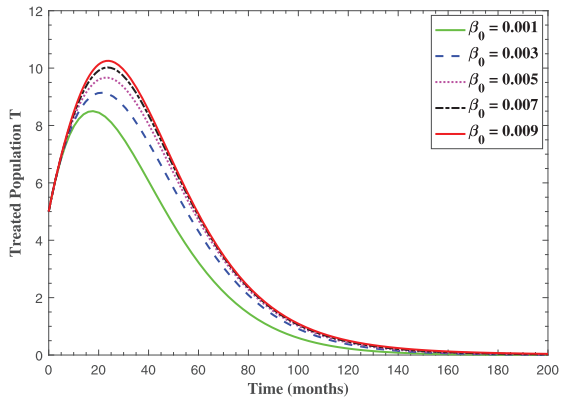

(e) Treated Population

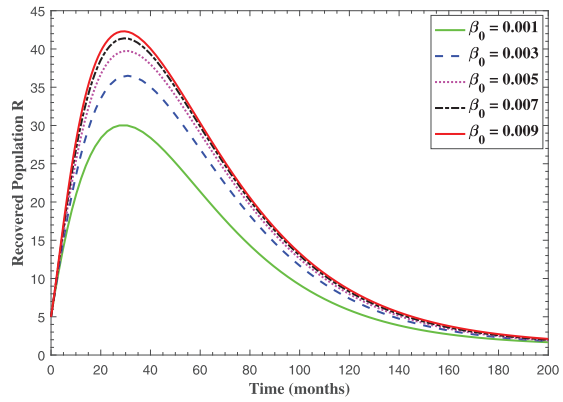

(f) Recovered Population

Figure 8: The graphs show the simulation results of $\mathbb{S}(t)$, $\mathbb{E}(t)$, $\mathbb{I}(t)$, $\mathbb{C}(t)$, $\mathbb{T}(t)$, and $\mathbb{R}(t)$ respectively, with respect to various baseline transmission coefficient β_0, when all other parameters are kept fixed

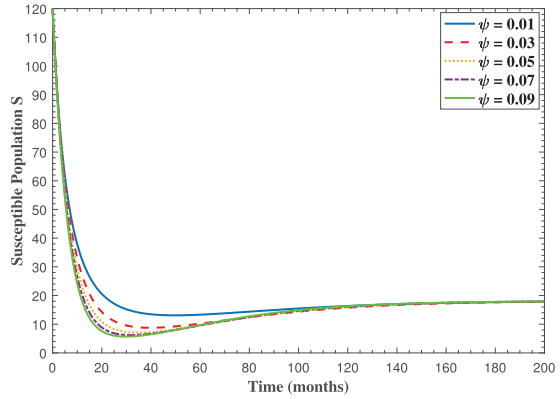

(a) Susceptible Population

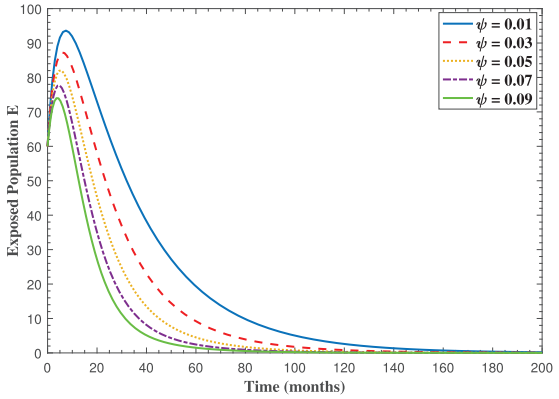

(b) Exposed Population

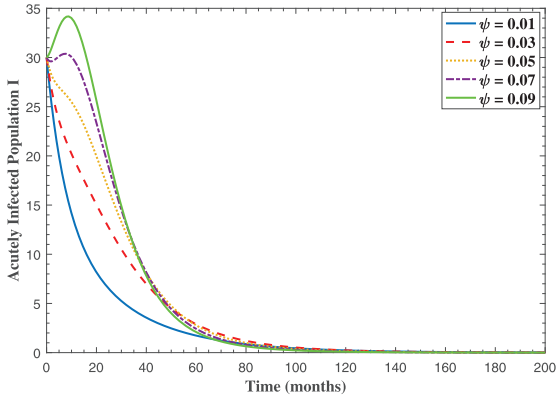

(c) Acutely Infected Population

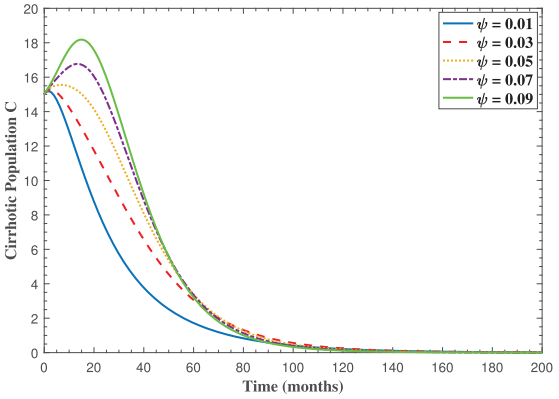

(d) Cirrhotic Population

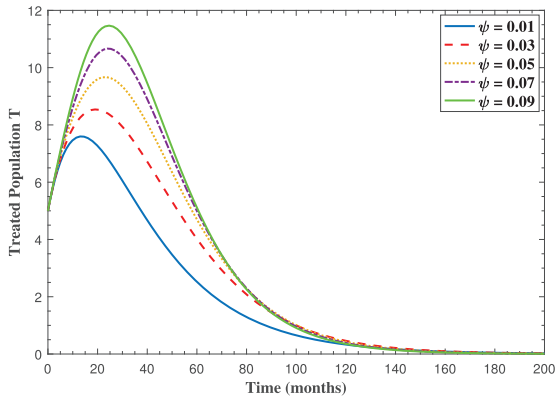

(e) Treated Population

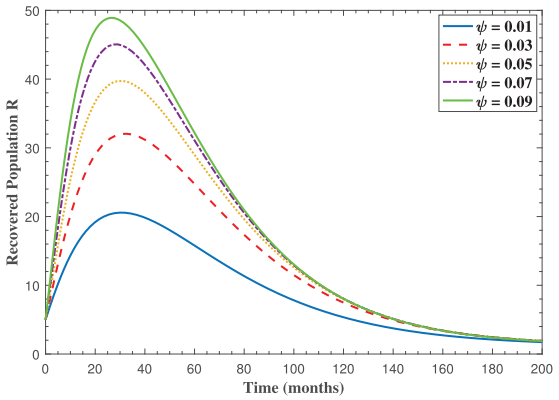

(f) Recovered Population

Figure 9: The graphs show the simulation results of $\mathbb{S}(t)$, $\mathbb{E}(t)$, $\mathbb{I}(t)$, $\mathbb{C}(t)$, $\mathbb{T}(t)$, and $\mathbb{R}(t)$ respectively, with respect to various acute infection transmission rate ψ, when all other parameters are kept fixed

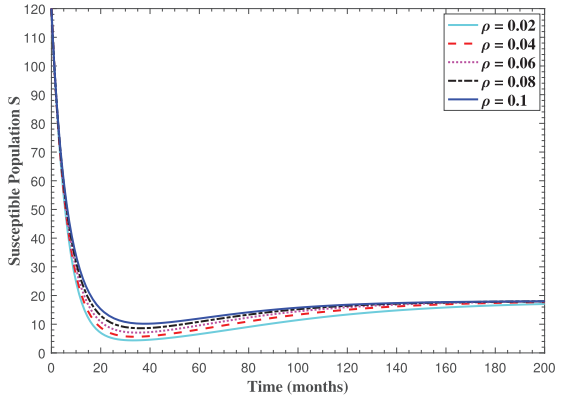

(a) Susceptible Population

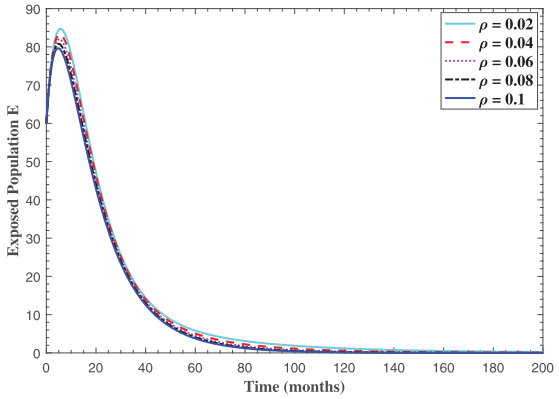

(b) Exposed Population

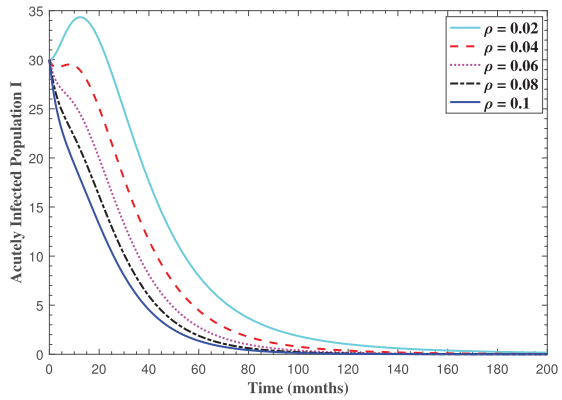

(c) Acutely Infected Population

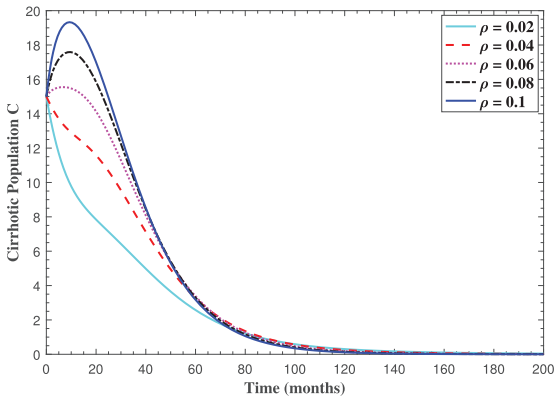

(d) Cirrhotic Population

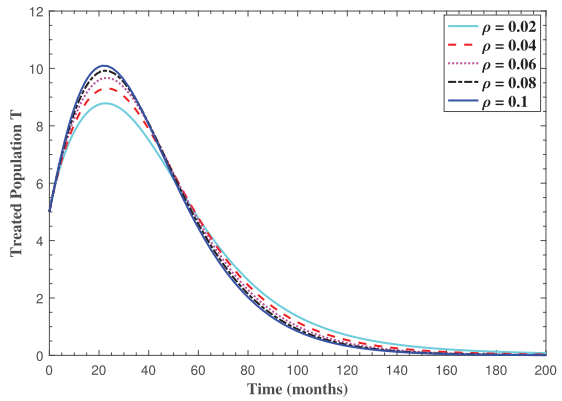

(e) Treated Population

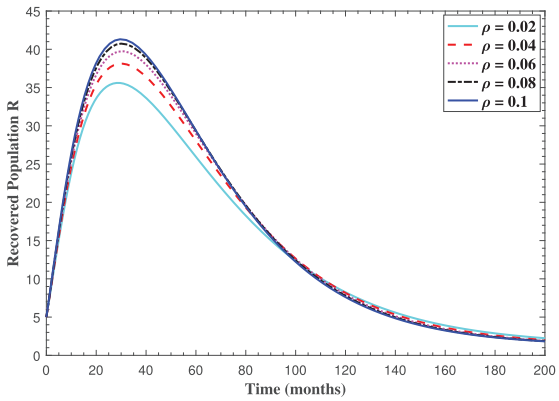

(f) Recovered Population

Figure 10: The graphs show the simulation results of $\mathbb{S}(t)$, $\mathbb{E}(t)$, $\mathbb{I}(t)$, $\mathbb{C}(t)$, $\mathbb{T}(t)$, and $\mathbb{R}(t)$ respectively, with respect to various cirrhosis progression rate ρ, when all other parameters are kept fixed

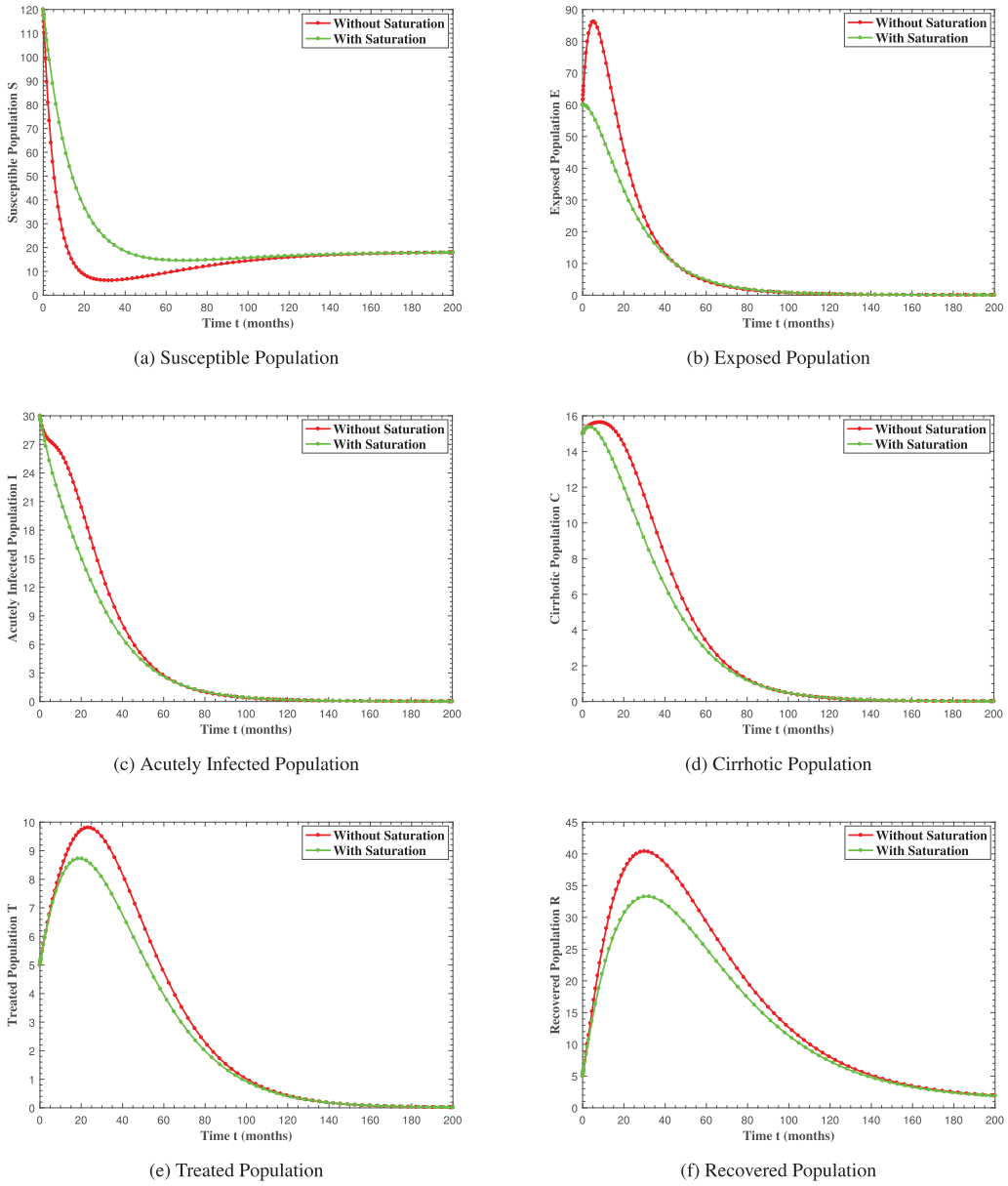

(a) Susceptible Population

(b) Exposed Population

(c) Acutely Infected Population

(d) Cirrhotic Population

(e) Treated Population

(f) Recovered Population

Figure 11: The graphs show the simulation results of $\mathbb{S}(t)$, $\mathbb{E}(t)$, $\mathbb{I}(t)$, $\mathbb{C}(t)$, $\mathbb{T}(t)$ and $\mathbb{R}(t)$ respectively, with saturation and without saturation

Fig. 12 represents the phase portrait of (a) $\mathbb{C}(t)$ vs. $\mathbb{I}(t)$, (b) $\mathbb{A}(t)$ vs. $\mathbb{E}(t)$, (c) $\mathbb{A}(t)$ vs. $\mathbb{I}(t)$, (d) $\mathbb{A}(t)$ vs. $\mathbb{C}(t)$, (e) $\mathbb{R}(t)$ vs. $\mathbb{E}(t)$ and (f) $\mathbb{T}(t)$ vs. $\mathbb{C}(t)$ with stable disease-free equilibrium and respective values of parameters in Table 1. In Fig. 12a, whenever the number of acutely infected individuals increases, the cirrhotic also increases for the first few months but then sharply converges to zero (the disease-free equilibrium). In Fig. 12b–d, as alcohol consumption increases, the exposed, acutely infected and cirrhotic individuals also increase, respectively for the first few months and start declining afterwards. Fig. 12e demonstrates that, for the first few months, whenever the number of exposed individuals increases, the recovered also increases slightly, but as the exposed individuals start declining, the recovered increases highly and converges to the disease-free equilibrium afterwards. Fig. 12f, shows that whenever the number

of cirrhotic people increases, the number of treated people also increases for the first few months, but after some time, both start to decline and converge to the disease-free equilibrium point. Similarly, Fig. 13 shows the phase space diagram of $(a)\ \mathbb{S}(t)$ vs. $\mathbb{R}(t)$, $(b)\ \mathbb{S}(t)$ vs. $\mathbb{C}(t)$, $(c)\ \mathbb{S}(t)$ vs. $\mathbb{E}(t)$, $(d)\ \mathbb{S}(t)$ vs. $\mathbb{I}(t)$, (e) $\mathbb{T}(t)$ vs. $\mathbb{I}(t)$ and $(f)\ \mathbb{R}(t)$ vs. $\mathbb{T}(t)$ with stable disease-free equilibrium and respective values of parameters in Table 1.

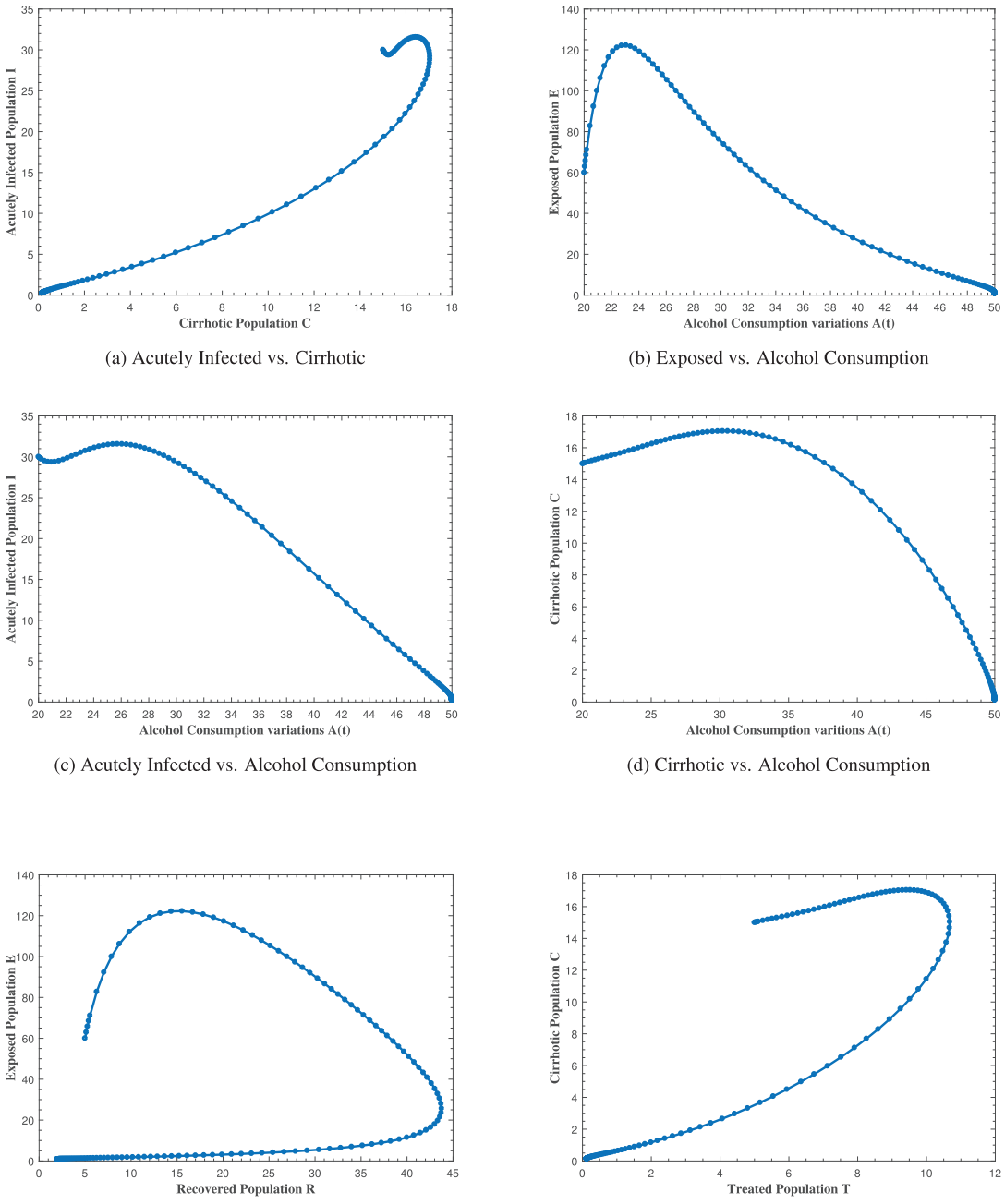

(a) Acutely Infected vs. Cirrhotic

(b) Exposed vs. Alcohol Consumption

(c) Acutely Infected vs. Alcohol Consumption

(d) Cirrhotic vs. Alcohol Consumption

(e) Exposed vs. Recovered

(f) Cirrhotic vs. Treated

Figure 12: The plot shows the phase space diagram of (**a**) $\mathbb{C}(t)$ vs. $\mathbb{I}(t)$, (**b**) $\mathbb{A}(t)$ vs. $\mathbb{E}(t)$, (**c**) $\mathbb{A}(t)$ vs. $\mathbb{I}(t)$, (**d**) $\mathbb{A}(t)$ vs. $\mathbb{C}(t)$, (**e**) $\mathbb{R}(t)$ vs. $\mathbb{E}(t)$ and (**f**) $\mathbb{T}(t)$ vs. $\mathbb{C}(t)$ with stable disease-free equilibrium

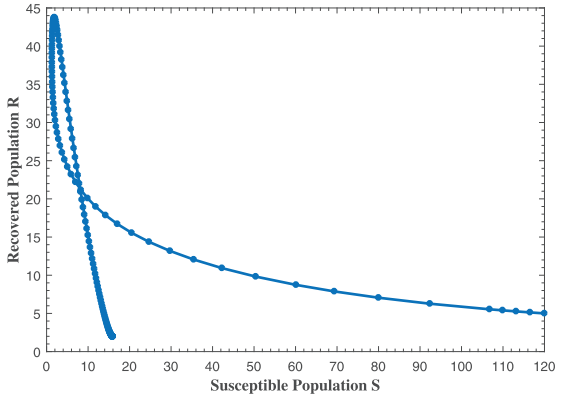

(a) Recovered vs. Susceptible

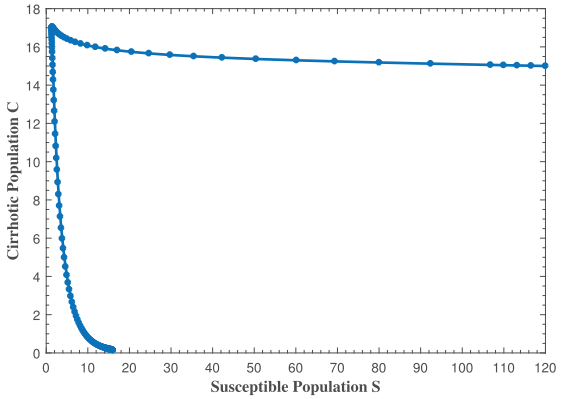

(b) Cirrhotic vs. Susceptible

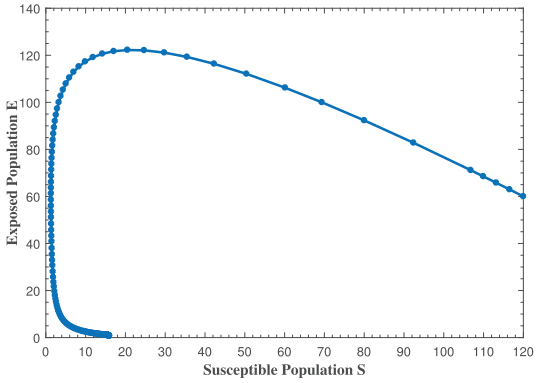

(c) Exposed vs. Susceptible

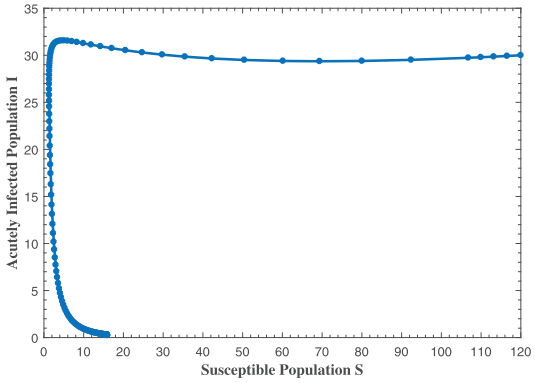

(d) Acutely Infected vs. Susceptible

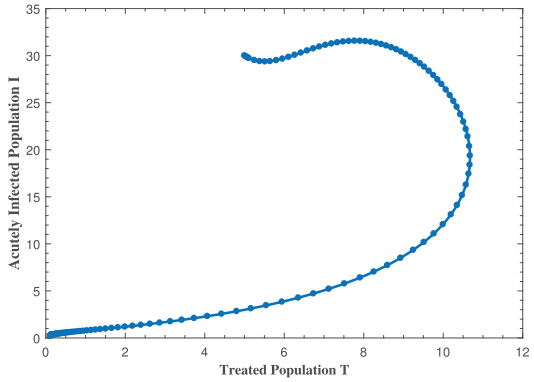

(e) Acutely Infected vs. Treated

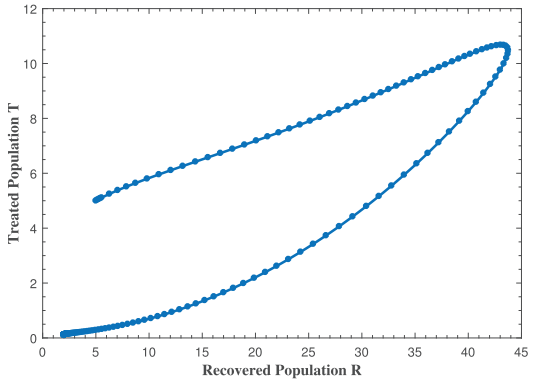

(f) Treated vs. Recovered

Figure 13: The plot shows the phase space diagram of (**a**) $\mathbb{S}(t)$ vs. $\mathbb{R}(t)$, (**b**) $\mathbb{S}(t)$ vs. $\mathbb{C}(t)$, (**c**) $\mathbb{S}(t)$ vs. $\mathbb{E}(t)$, (**d**) $\mathbb{S}(t)$ vs. $\mathbb{I}(t)$, (**e**) $\mathbb{T}(t)$ vs. $\mathbb{I}(t)$ and (**f**) $\mathbb{R}(t)$ vs. $\mathbb{T}(t)$ with stable disease-free equilibrium

In Fig. 14, the system (1) reaches endemic state by assuming $b = 0.98$, $\beta_0 = 0.04$, $\beta_1 = 0.14$, $\mu_0 = 0.01$ $\nu = 0.02$, $\rho = 0.25$, $\gamma_1 = 0.89$, $\tau_1 = 0.15$, and $\psi = 0.2$ with all other parameter values in Table 1, which results $\mathscr{R}_0 = [\mathscr{R}_{A_0}, \mathscr{R}_{A_{max}}] > 1$. The susceptible population decreases while all other populations increase, but this pattern persists for a specific duration. After some time, all the trajectories of the system states converge to

the endemic equilibrium point. In both figures, all curves remain at these specific values when high or low amount of alcohol is consumed, confirming the stability of the endemic equilibrium point of system (1).

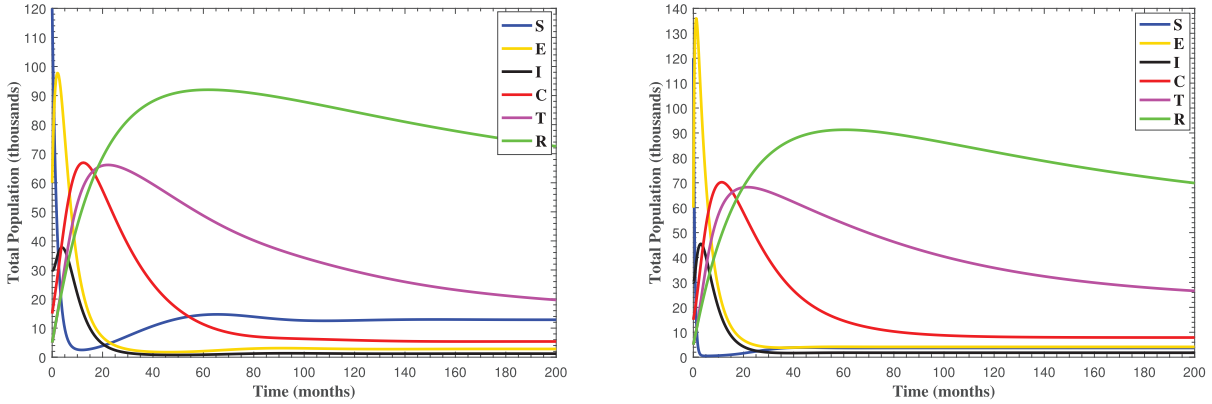

(a) When alcohol consumption is $\mathbb{A}(t) = A_0$ and $\mathscr{R}_{A_0} = 2.688242 > 1$

(b) When alcohol consumption is $\mathbb{A}(t) = A_{max}$ and $\mathscr{R}_{A_{max}} = 9.588 > 1$

Figure 14: The plots shows how all trajectories of the state variables $\mathbb{S}(t), \mathbb{E}(t), \mathbb{I}(t), \mathbb{C}(t), \mathbb{T}(t)$ and $\mathbb{R}(t)$ converging to endemic equilibrium

8 Conclusion

In this study, the combined effect of heavy alcohol use and Hepatitis B infection on the dynamics of liver cirrhosis development was examined using the idea of a deterministic epidemiological model. A logistic equation was also employed to explain the variability in alcohol intake over time. This model helped in understanding and analyzing various dynamical properties of the combined effect of heavy alcohol use and Hepatitis B infection. In addition, we considered the saturated incidence rate and showed the effect of the saturation parameter on each class. Moreover, a treated compartment was added to see the complex relationships among liver cirrhosis, recovery, and therapy dynamics. The basic characteristics of the proposed model were examined to confirm its viability both mathematically and biologically. The basic reproductive numbers $\mathscr{R}_{A_0}$ and $\mathscr{R}_{A_{max}}$ and the equilibria for both the disease-free and endemic are obtained, as well as the local and global stabilities of the equilibria. The sensitivity analysis was performed and demonstrated the role of every parameter and quantified the most sensitive parameters to the liver cirrhosis transmission. Using central manifold theory and the method of Chavez & Song, we established and proved the existence of forward bifurcation. Ultimately, detailed numerical simulations were conducted for the suggested model, confirming the analytical results. The numerical simulation results reveal that if an alcohol usage reduction program is not implemented, the effects of the combination of heavy alcohol use and Hepatitis B infection will accelerate the progression of liver cirrhosis. However, inhibitory or crowding effects of susceptible and infected individuals, respectively, and treatment of acutely infected individuals may reduce liver cirrhosis progression.

To eradicate liver cirrhosis in the community, any committed researcher is encouraged to apply an optimal control strategy by considering different control variables to reduce the risk of alcohol intake in chronic Hepatitis B carriers. The most significant factor in Hepatitis B transmission is age dependency. Therefore, the same model can be converted into an age-structured model to see the effects of Hepatitis B and liver cirrhosis on different age groups. Furthermore, the same model can be converted to a stochastic model to study random fluctuations and uncertainty in liver cirrhosis progression dynamics.

This study has certain limitations that provide avenues for future research. While the model captures the synergistic dynamics of Hepatitis B and alcohol, it does not incorporate spatial heterogeneity, despite the well-documented geographical variability in Hepatitis B prevalence and alcohol consumption patterns. The current deterministic framework was chosen to establish a foundational, analytically tractable understanding of the core mechanisms. The exclusion of spatial effects allows for a focused analysis on the population-level interactions between disease progression and behavioral factors without the added complexity of regional parameterization and human mobility networks. Future work will aim to extend this model into a spatial or meta-population framework to explore how regional differences in public health policies, vaccination coverage, and cultural norms regarding alcohol use influence the overall burden of liver cirrhosis.

Acknowledgement: Not applicable.

Funding Statement: No funding was received to assist with the preparation of this manuscript.

Author Contributions: Zia Ur Rahman, Formal Analysis; Nigar Ali, Zeeshan Ali, Conceptualization; Dragan Pamucar, Review and Editing; Imtiaz Ahmad, Simulation and Validation; Haci Mehmet Baskonus, Overall Supervision and Review, Naseer Ul Haq, Writing Original Draft; Zeeshan Ali, Methodology, Validation, Resources. All authors reviewed the results and approved the final version of the manuscript.

Availability of Data and Materials: All data that support the findings of this study are included within the article.

Ethics Approval: Not applicable.

Conflicts of Interest: The authors declare no conflicts of interest to report regarding the present study.

References

1. Ginès P, Krag A, Abraldes JG, Solà E, Fabrellas N, Kamath PS. Liver cirrhosis. Lancet. 2021;398(10308):1359–76.
2. Khatun MS, Biswas MHA. Optimal control strategies for preventing hepatitis B infection and reducing chronic liver cirrhosis incidence. Infect Dis Model. 2020;5:91–110. doi:10.1016/j.idm.2019.12.006.
3. Canadian Centre for Occupational Health and Safety. Hepatitis B. Hamilton, ON, Canada: Canadian Centre for Occupational Health and Safety; 2024 [cited 2025 May 30]. Available from: www.ccohs.ca/oshanswers/diseases/hepatitisb.html.
4. Khan M, Khan T, Ahmad I, Shah Z, Khan A. Modeling of Hepatitis B virus transmission with fractional analysis. Math Probl Eng. 2022;2022(1):6202049.
5. World Health Organization. Hepatitis B [Fact sheet]. 2024 [cited 2025 Nov 11]. Available from: http://www.who.int/mediacentre/factsheets/fs204/en/.
6. Iida-Ueno A, Enomoto M, Tamori A, Kawada N. Hepatitis B virus infection and alcohol consumption. World J Gastroenterol. 2017;23(15):2651. doi:10.3748/wjg.v23.i15.2651.
7. Ganesan M, Eikenberry A, Poluektova LY, Kharbanda KK, Osna NA. Role of alcohol in pathogenesis of hepatitis B virus infection. World J Gastroenterol. 2020;26(9):883. doi:10.3748/wjg.v26.i9.883.
8. Din A, Li Y, Liu Q. Viral dynamics and control of hepatitis B virus (HBV) using an epidemic model. Alex Eng J. 2020;59(2):667–79. doi:10.1016/j.aej.2020.01.034.
9. Xu HQ, Wang CG, Zhou Q, Gao YH. Effects of alcohol consumption on viral hepatitis B and C. World J Clin Cases. 2021;9(33):10052. doi:10.12998/wjcc.v9.i33.10052.
10. Vonghia L, Leggio L, Ferrulli A, Bertini M, Gasbarrini G, Addolorato, Alcoholism Treatment Study Group. Acute alcohol intoxication. Eur J Internal Med. 2008;19(8):561–7. doi:10.1016/j.ejim.2007.06.033.
11. Khan T, Ullah R, Zaman G, Ahmad I. The analysis of hepatitis B virus (HBV) transmission using an epidemic model. Nat Appl Sci Int J (NASIJ). 2021;2(1):70–9. doi:10.47264/idea.nasij/2.1.6.

12. Lai CL, Yuen MF. The natural history and treatment of chronic hepatitis B: a critical evaluation of standard treatment criteria and end points. Ann Intern Med. 2007;147(1):58–61. doi:10.7326/0003-4819-147-1-200707030-00010.
13. Capasso V, Serio G. A generalization of the Kermack–McKendrick deterministic epidemic model. Math Biosci. 1978;42(1–2):43–61. doi:10.1016/0025-5564(78)90006-8.
14. Azeem M, Jamil MK. On the anticancer drug structures and their locating numbers. Spectrum Oper Res. 2024;1(1):44–63. doi:10.31181/sor1120245.
15. Azeem M, Jamil MK. Constant partition dimension of different anticancer drug structures. Spectrum Decis Making Appl. 2024;1(1):64–83. doi:10.31181/sdmap1120245.
16. Zhou L, Fan M. Dynamics of an SIR epidemic model with limited medical resources revisited. Nonlinear Anal: Real World Appl. 2012;13(1):312–24. doi:10.1016/j.nonrwa.2011.07.036.
17. Ilhan Ö, Şahin G. A numerical approach for an epidemic SIR model via Morgan-Voyce series. Int J Math Comput Eng. 2024;2(1):125–40. doi:10.2478/ijmce-2024-0010.
18. Park B, Jung KW, Oh CM, Choi KS, Suh M, Jun JK. Factors associated with alcohol consumption in hepatitis B carriers: a nationwide study in the Republic of Korea. PLoS One. 2014;9(11):e110144. doi:10.1371/journal.pone.0110144.
19. Khajji B, Labzai A, Balatif O, Rachik M. Mathematical modeling and analysis of an alcohol drinking model with the influence of alcohol treatment centers. Int J Math Math Sci. 2020;2020(1):4903168. doi:10.1155/2020/4903168.
20. Shah I, Ali I, Ali A, Ahmad I, Islam S, Rasool G, et al. Optimal control and sensitivity analysis of a mathematical model for MDR-TB transmission with advanced treatment strategies. Eur Phys J Plus. 2025;140(6):1–15. doi:10.1140/epjp/s13360-025-06486-8.
21. Chawla SR, Ahmad S, Albalawi W, Khan A, Shah I, Eid MR. Stability analysis of a modified general *SEIR* model with harmonic mean type of incidence rate. Alexandria Eng J. 2025;127:1183–92. doi:10.1016/j.aej.2025.07.006.
22. Zhou E, Yang C, Gao Y. Effect of alcohol on the progress of hepatitis B cirrhosis. Ann Palliat Med. 2021;10(1):415–24. doi:10.21037/apm-20-2353.
23. Dano LB, Rao KP, Keno TD. Modeling the combined effect of hepatitis B infection and heavy alcohol consumption on the progression dynamics of liver cirrhosis. J Math. 2022;2022(1):6936396. doi:10.1155/2022/6936396.
24. Izgi ZP. Simulation studies on the hemodynamic model for blood flow. Int J Math Comput Eng. 2024;3(1):75–82. doi:10.2478/ijmce-2025-0007.
25. Farhan M, Shah Z, Ling Z, Shah K, Abdeljawad T, Islam S, et al. Global dynamics and computational modeling for analyzing and controlling hepatitis B: a novel epidemic approach. PLoS One. 2024;19(6):e0304375. doi:10.1371/journal.pone.0304375.
26. Bruha R, Dvorak K, Petrtyl J. Alcoholic liver disease. World J Hepatol. 2012;4(3):81.
27. Ullah I, Ahmad I, Ali N, Ahmad H, Haq IU. Mathematical modeling and analysis of dynamics of neisseria gonorrhea disease with self-protection, treatment and natural immunity. Glob J Sci. 2024;1(1):40–55. doi:10.48165/gjs.2024.1105.
28. Van den Driessche P, Watmough J. Reproduction numbers and sub-threshold endemic equilibria for compartmental models of disease transmission. Math Biosci. 2002;180(1–2):29–48. doi:10.1016/s0025-5564(02)00108-6.
29. Khan MA, DarAssi MH, Ahmad I, Seyam NM, Alzahrani E. Modeling the dynamics of tuberculosis with vaccination, treatment, and environmental impact: fractional order modeling. Comput Model Eng Sci. 2024;141(2):1365–94. doi:10.32604/cmes.2024.053681.
30. Ndendya JZ, Leandry L, Kipingu AM. A next-generation matrix approach using Routh-Hurwitz criterion and quadratic Lyapunov function for modeling animal rabies with infective immigrants. Healthcare Anal. 2023;4:100260. doi:10.1016/j.health.2023.100260.
31. Mahardika R, Widowati, Sumanto YD. Routh-hurwitz criterion and bifurcation method for stability analysis of tuberculosis transmission model. J Phys Conf Series. 2019;1217(1):012056. doi:10.1088/1742-6596/1217/1/012056.
32. Jehangir H, Ali N, Ahmad I, Younas H, Ahmad Z, El-Agamy RF. Global dynamics and numerical simulation of a vaccinated mathematical model for rabies disease. Glob J Sci. 2024;1(1):14–27.

33. LaSalle JP. Stability theory and invariance principles. In: Dynamical systems. New York, NY, USA: Academic Press; 1976. p. 211–22.
34. Vanderbauwhede A, Iooss G. Center manifold theory in infinite dimensions. In: Dynamics reported: expositions in dynamical systems. Berlin/Heidelberg, Germany: Springer; 1992. p. 125–63.
35. Castillo-Chavez C, Song B. Dynamical models of tuberculosis and their applications. Math Biosci Eng. 2004;1(2):361–404. doi:10.3934/mbe.2004.1.361.
36. Buonomo B, Lacitignola D. On the backward bifurcation of a vaccination model with nonlinear incidence. Nonlinear Anal Model Control. 2011;16(1):30–46. doi:10.15388/NA.16.1.14113.
37. Chitnis N, Hyman JM, Cushing JM. Determining important parameters in the spread of malaria through the sensitivity analysis of a mathematical model. Bull Math Biol. 2008;70:1272–96. doi:10.1007/s11538-008-9299-0.